bioRxiv preprint doi: https://doi.org/10.1101/2021.05.31.446416; this version posted October 26, 2021. The copyright holder for this preprint (which was not certified by peer review) is the author/funder, who has granted bioRxiv a license to display the preprint in perpetuity. It is made available under a CC-BY-ND 4.0 International license.

Nuclear and plastid phylogenomic analyses provide insights into the reticulate evolution, species delimitation and biogeography of the Sino-Japanese disjunctive *Diabelia* (Caprifoliaceae)

Xiu-Rong Ke[a], Diego F. Morales-Briones[b,c], Hong-Xin Wang[a,d], Qing-Hui Sun[a], Jacob B. Landis[e,f], Jun Wen[g], Hua-Feng Wang[a]*

[a] *Key Laboratory of Tropical Biological Resources of Ministry of Education, College of Tropical Crops, Hainan University, Haikou 570228, China*

[b] *Department of Plant and Microbial Biology, College of Biological Sciences, University of Minnesota, 140 Gortner Laboratory, 1479 Gortner Avenue, Saint Paul, MN 55108, USA*

[c] *Systematics, Biodiversity and Evolution of Plants, Department of Biology I, Ludwig-Maximilians-Universität München, Menzinger Str. 67, 80638, Munich, Germany*

[d] *Zhai Mingguo Academician Work Station, Sanya University, Sanya 572022, China*

[e] *School of Integrative Plant Science, Section of Plant Biology and the L.H. Bailey Hortorium, Cornell University, Ithaca, NY 14850, USA*

[f] *BTI Computational Biology Center, Boyce Thompson Institute, Ithaca, NY 14853, USA*

[g] *Department of Botany, National Museum of Natural History, MRC-166, Smithsonian*

*Authors for correspondence:

Hua-Feng Wang, E-mail: hfwang@hainanu.edu.cn

bioRxiv preprint doi: https://doi.org/10.1101/2021.05.31.446416; this version posted October 26, 2021. The copyright holder for this preprint (which was not certified by peer review) is the author/funder, who has granted bioRxiv a license to display the preprint in perpetuity. It is made available under a CC-BY-ND 4.0 International license.

Abstract: Understanding biological diversity and the mechanisms of the Sino-Japanese disjunctions are major challenges in eastern Asia biogeography. The Sino-Japanese flora has been broadly studied as an ideal model for plant phylogeography. *Diabelia* (Caprifoliaceae) is an East Asian genus, with a disjunctive distribution across the Sino-Japanese region. However, relationships within *Diabelia* remain elusive. In this study, we reconstructed the phylogeny of *Diabelia* and inferred historical biogeography and evolutionary patterns based on nuclear and plastid sequences from target enrichment and genome skimming approaches, respectively. We found that the main clades within *Diabelia* were discordant between nuclear and plastid trees. Both nuclear and plastid phylogenetic analyses supported five main clades: *D. serrata*, *D. tetrasepala*, *D. sanguinea*, *D. spathulata* var. *stenophylla* and *D. spathulata* var. *spathulata*. Species network analyses revealed that *Diabelia tetrasepala* is likely the result of a hybridization event. Divergence time estimation and ancestral area reconstructions showed that *Diabelia* originated in Japan during the early Miocene, with subsequent vicariance and dispersal events between Japan and Korea, and between Japan and China. Overall, our results support the division of *Diabelia* into five main clades and the recognition of five species in the genus. This research provides new insights in the species delimitation and speciation processes of taxonomically complex lineages such as *Diabelia*.

Keywords: *Diabelia;* Phylogenomics; Gene tree discordance; Cytonuclear discordance; Hybridization

bioRxiv preprint doi: https://doi.org/10.1101/2021.05.31.446416; this version posted October 26, 2021. The copyright holder for this preprint (which was not certified by peer review) is the author/funder, who has granted bioRxiv a license to display the preprint in perpetuity. It is made available under a CC-BY-ND 4.0 International license.

1 Introduction

Understanding how different factors have shaped current biological diversity is a major challenge for evolutionary biology (Jiang et al., 2016; Casebolt & Kowalewski, 2018; Wang et al., 2018; Martínez-Espinosa, 2021; Maguilla et al., 2021). The Sino-Japanese floristic region (SJFR) of East Asia was an important glacial sanctuary during the Quaternary and harbors the highest diversity of temperate plant species in the world, warranting much attention to understand its origin and diversification (Mitsui et al., 2008; Qiu et a1., 2009; 2011; Zhao et al., 2019; Tian et al. 2020; Zhang et al., 2020). The SJFR extends widely over an area from southwest China to northern Japan, with complex topography and multiple climatic zones (Qiu et a1., 2011; Lu et al., 2020). The eastern edge of the SJFR experienced dramatic changes in the palaeo-landscape during the Miocene and Pliocene (Ota, 1988; Lu et al., 2020), which may have played key roles in isolating ancient Japanese plant species from continental East Asian species.

Diabelia Landrein (Caprifoliaceae) is an East Asian endemic genus and was recently segregated from *Abelia* based on the paired flowers appearing at the end of short shoots (Landrein, 2010; Wang et al., 2020). This genus of shrubs belongs to the subfamily Linnaeoideae (Landrein, 2010; Wang et al., 2015; Landrein and Farjon, 2020; Wang et al., 2020) and traditionally included three species: *Diabelia serrata* (Siebold & Zucc.) Landrein with two sepals, *D. tetrasepala* (Koidz.) Landrein with four big and one smaller sepal, and *D. spathulata* (Siebold & Zucc.) Landrein with five sepals, which is further subdivided into three varieties, var. *spathulata*, var. *sanguinea* (Makino) Landrein, and var. *stenophylla* (Honda) Landrein (Fig. 1; Hara, 1983). *Diabelia* shows a disjunct distribution in the SJFR (Hara, 1983; Landrein, 2010; Zhao et al., 2019; Landrein and Farjon, 2020; Wang et al., 2020): *D. serrata* is widely distributed in southern Japan as well as on the southeastern coast of China; *D. spathulata* is distributed in south, central and northern areas of Japan, but rare in China and Korea; *D. tetrasepala* is distributed in the area from Fukushima to Fukuoka Prefectures in Japan, and its distribution range partly overlaps with that of *D.*

bioRxiv preprint doi: https://doi.org/10.1101/2021.05.31.446416; this version posted October 26, 2021. The copyright holder for this preprint (which was not certified by peer review) is the author/funder, who has granted bioRxiv a license to display the preprint in perpetuity. It is made available under a CC-BY-ND 4.0 International license.

spathulata and *D. serrata*. Based on morphological characters (the number of sepals, nectary cushion position, and corolla color), Landrein and Farjon (2020) have proposed the recognition of four species: *D. serrata*, *D. spathulata*, *D. sanguinea* (Makino) Landrein, and *D. stenophylla* (Honda) Landrein.

There have been several previous studies on disjunct distributions between China and Japan (e.g., Lu et al., 2020; Haq et al., 2020; Takano et al., 2020), with most studies focusing on species that are widely distributed in Japan. Disjunct distribution patterns typically have been attributed to vicariance or long-distance dispersal events (Doyle et al., 2004; Baenfer et al., 2006; Bobo-Pinilla et al., 2018; Torres-Cambas et al., 2019; Wang et al., 2020; Nge et al., 2021). The disjunct distribution of *Diabelia* can be dated back to the middle Oligocene, spanning the long geological history of the formation of the flora in China and Japan (Yang et al., 2011; Shin et al., 2012; Zhao et al., 2019; Wang et al., 2020; Zhang et al., 2020). Overall, exploring the internal phylogenetic relationships and biogeographic diversification of *Diabelia* is conducive for further inference of the mechanisms leading to the disjunct distribution of SJFR in East Asia.

Several previous molecular phylogenetic studies have been conducted on *Diabelia* (Zhou et al., 2004; Landrein et al., 2012; Wang et al., 2015). However, relationships within *Diabelia* remain controversial due to limited markers and sampling. Zhou et al. (2004) conducted an Amplified Fragment Length Polymorphism (AFLP) analysis including six *Diabelia* samples and found that *D. serrata* from China was closely related to accessions of the same species from Japan. Using the nuclear internal transcribed spacer (ITS) and plastid markers (*rbcL, ndhF, matK, trnL* intron and *trnL-F* intergenic spacer), Landrein et al. (2012) found a close relationship between *D. serrata* and *D. spathulata*. Based on nine plastid markers, Wang et al. (2015) constructed a phylogeny recovering a close relationship of *D. serrata* between China and Japan. Subsequent molecular phylogenetic studies have enriched sampling across the SJFR to further investigate the phylogenetic relationships within *Diabelia*. Using plastid fragments from 37 *Diabelia* samples, Zhao et al. (2019) found the non-monophyly of several *Diabelia* species. Yet based on complete plastomes, Wang et

bioRxiv preprint doi: https://doi.org/10.1101/2021.05.31.446416; this version posted October 26, 2021. The copyright holder for this preprint (which was not certified by peer review) is the author/funder, who has granted bioRxiv a license to display the preprint in perpetuity. It is made available under a CC-BY-ND 4.0 International license.

al. (2020) recovered the monophyly of *D. serrata* while the relationships of the other species remained unresolved. Overall, sufficient informative molecular data from both nuclear and plastid genomes and a large taxonomic sampling are essential for the comprehensive reconstruction of phylogenetic relationships within *Diabelia*.

Organelle genes often exhibit phylogenetic patterns significantly different from nuclear markers (Toews and Brelsford, 2012; Leducq et al., 2017; Ji et al., 2019; Yao et al., 2019; Wang et al., 2021). Currently, target enrichment is emerging as the method of choice to obtain target sequence for numerous nuclear orthologs of many complex taxa (Wanke et al., 2017; Buys et al., 2019; Schneider et al., 2020; Granados Mendoza et al., 2020; Wang et al., 2021). Many studies have applied this method to obtain data sets for analyzing cyto-nuclear discordance, speciation, hybridization, and polyploidy (e.g., Bogarin et al., 2018; Morales-Briones et al., 2018; 2021). Given that the species-level phylogeny of *Diabelia* has remained largely unresolved, we obtained data through target enrichment and genome skimming of broadly sampled *Diabelia* accessions across the SJFR, which allowed us to (1) robustly explore intrageneric phylogenetic relationships and compare them against previous phylogenies, and (2) to elucidate the biogeography and evolution of the genus to offer a comprehensive phylogenetic framework for future studies.

2 Materials and Methods

2.1 Sampling

A data set of 47 accessions was analyzed including 42 *Diabelia* samples (encompassing all four currently recognized species of *Diabelia* and one variety of *Diabelia stenophylla* (Honda) Landrein var. *tetrasepala* (Koidz.) Landrein) (Landrein et al., 2012; Zhao et al. 2019; Landrein and Farjon, 2020; Wang et al., 2020) and five outgroup samples representing Linnaeoideae (*Abelia macrotera* var. *macrotera*, *Dipelta floribunda* Maxim., *Kolkwitzia amabilis* Graebn., *Vesalea floribunda* M.Martens & Galeotti, *Linnaea borealis* L.). Voucher specimens have been deposited in the herbarium of the Institute of Tropical Agriculture and Forestry of Hainan

bioRxiv preprint doi: https://doi.org/10.1101/2021.05.31.446416; this version posted October 26, 2021. The copyright holder for this preprint (which was not certified by peer review) is the author/funder, who has granted bioRxiv a license to display the preprint in perpetuity. It is made available under a CC-BY-ND 4.0 International license.

University (HUTB), Haikou, China. Detailed information on the geographical distribution and voucher details for the 47 samples and the localities of the populations sampled in this study are shown in Table S1.

2.2 DNA extraction and sequencing

We used a modified CTAB method (Doyle & Doyle, 1987) to extract total genomic DNA from silica gel-dried tissue or herbarium accessions. The concentration of each extraction was checked with a Qubit 2.0 Fluorometer (Thermo Fisher Scientific, Waltham, MA, USA). A total of 400 ng of DNA was sonicated with a Covaris S2 (Covaris, Woburn, MA) to produce fragments ~150-350 bp in length prior to library preparation. Libraries of genomic DNA were made following Weitemier et al. (2014). To ensure that genomic DNA was sheared to the appropriate fragment size, all samples were evaluated on a 1.2% (w/v) agarose gel.

To obtain nuclear data we used a target enrichment approach (Weitemier et al., 2014) and plastid data we used genome skimming (Wang et al., 2020). Baits designed across Dipsacales (Wang et al., 2021) were used to target 428 putatively single-copy genes. Hybridization, enrichment, and sequencing followed Wang et al. (2021).

2.3 Reads processing and assembly

Trimmomatic v.0.36 (Bolger et al., 2014) was used to remove adaptor sequences and low-quality bases from the raw reads (ILLUMINACLIP: TruSeq_ADAPTER: 2:30:10 SLIDINGWINDOW: 4:5 LEADING: 5 TRAILING: 5 MINLEN: 25). HybPiper v.1.3.1 (Johnson et al., 2016) was employed to assemble the nuclear loci. Exons were assembled individually to avoid chimeric sequences in multi-exon genes produced by potential paralogy (Morales-Briones et al., 2018), in which exons longer than 150 bp were set as a reference. Paralog detection was undertaken for all exons using the 'paralog_investigator' option in HybPiper. To obtain 'monophyletic outgroup'(MO) orthologs (Yang and Smith, 2014), all assembled loci (with and without paralogs detected) were processed following Morales-Briones et al. (2021).

bioRxiv preprint doi: https://doi.org/10.1101/2021.05.31.446416; this version posted October 26, 2021. The copyright holder for this preprint (which was not certified by peer review) is the author/funder, who has granted bioRxiv a license to display the preprint in perpetuity. It is made available under a CC-BY-ND 4.0 International license.

For the plastome assemblies, clean reads were extracted from the raw sequencing reads by using SOAPfilter_v2.2 to remove adapter sequences and low-quality reads. The resulting reads were used as the input to assemble plastomes using MITObim v1.8 (Hahn et al. 2013) following Wang et al. (2020).

2.4 Phylogenetic analyses

Nuclear data sets. We used concatenation and coalescent-based methods to analyze the nuclear data. For concatenation analyses, sequences of individual nuclear exons were aligned with MAFFT v.7.407 (Katoh & Standley, 2013) and columns with more than 90% missing data were removed using Phyutility (Smith and Dunn, 2008). A maximum likelihood tree from the concatenated matrix was inferred with RAxML v.8.2.20 (Stamatakis, 2014) using a partition-by-locus scheme and the GTRGAMMA substitution model for all partitions. We assessed clade support with 100 rapid bootstrap replicates (BS). For coalescent species tree estimation, ASTRAL-III v.5.7.1 (Zhang et al., 2018) was used to estimate a species tree based on individual exon trees constructed using RAxML with a GTRGAMMA model. We used local posterior probabilities (LPP) to calculate branch support (Sayyari and Mirarab, 2016). To evaluate nuclear gene tree discordance, we used Quartet Sampling (QS; Pease et al., 2018) to distinguish strong conflict from weakly supported branches with 1000 replicates. Additionally, we calculated the internode certainty all (ICA) score (Salichos et al., 2014) and the number of conflicting and concordant bipartitions on each node of the species trees with Phyparts (Smith et al., 2015).

Plastome data set. Complete plastomes were aligned using MAFFT v.7.407 (Katoh and Standley, 2013). A ML tree was inferred with IQ-TREE v.1.6.1 (Nguyen et al., 2015) under the extended model and 200 non-parametric BS replicates for branch support. In addition, branch support was evaluated using QS with 1000 replicates.

2.5 Species network analysis

We used PhyloNet (Wen et al., 2018) to infer a maximum pseudo-likelihood

bioRxiv preprint doi: https://doi.org/10.1101/2021.05.31.446416; this version posted October 26, 2021. The copyright holder for this preprint (which was not certified by peer review) is the author/funder, who has granted bioRxiv a license to display the preprint in perpetuity. It is made available under a CC-BY-ND 4.0 International license.

species network with the InferNetwork_MPL command (Yu and Nakhleh, 2015). Due to computational restrictions and given that we were primarily concerned with the underlying network between different species, we reduced the 47-taxon data set to one outgroup and 14 ingroup taxa to represent all major clades within *Diabelia*. Network searches were undertaken using only nodes in the gene trees that had at least 50% bootstrap support, allowing up to five hybridization events while optimizing branch lengths and inheritance probabilities of the returned species networks under the full likelihood. The command 'CalGTProb' in PhyloNet was used to infer the maximum likelihood of the concatenated RAxML, ASTRAL, and plastid trees, given the individual gene trees to estimate the optimal number of hybridization events and inspect whether the species network represented a better model than a purely bifurcating tree. The bias-corrected Akaike information criterion (AICc; Sugiura, 1978), Akaike information criterion (AIC; Akaike, 1973), and Bayesian information criterion (BIC; Schwarz, 1978) were used for model selection, with the best-fit-species network having the lowest AICc, AIC and BIC scores.

2.6 Divergence time estimation

Divergence times were estimated with BEAST v.2.4.0 (Bouckaert et al., 2014) using the concatenated nuclear data set. The root age was set to 50 Ma (lognormal prior distribution 32.66 - 57.81 Ma) following Wang et al. (2021). We selected the fruit fossil of *Diplodipelta* Manchester & Donoghue (Bell & Donoghue, 2005) that could confidently be placed in our tree as an internal calibration point, with the constraint set to 36 Ma (offset 36 Ma, lognormal prior distribution 34.07 - 37.20 Ma). Dating analyses were carried out using an uncorrelated lognormal relaxed clock under the GTR + G model for each marker partitioned separately and a Yule tree prior. The MCMC chains were run for 500,000,000 generations and sampling every 5,000 generations. Tracer v.1.7 (Drummond et al., 2012) was used to check convergence with the first 10% of trees removed as burn-in and to assess that all effective sample size (ESS) values were $\geqslant$ 200. The produced tree files were combined using

bioRxiv preprint doi: https://doi.org/10.1101/2021.05.31.446416; this version posted October 26, 2021. The copyright holder for this preprint (which was not certified by peer review) is the author/funder, who has granted bioRxiv a license to display the preprint in perpetuity. It is made available under a CC-BY-ND 4.0 International license.

LogCombiner v1.8.2 and the maximum clade credibility tree was generated in TreeAnnotator v1.8.4 (Drummond et al., 2012).

2.7 Ancestral area reconstruction

The ancestral area reconstruction was done using the Statistical Dispersal‐Vicariance Analysis (S‐DIVA) in RASP version 4.2 (Yu et al., 2015) based on Bayesian Binary Method (BBM) with the concatenated nuclear data set. To prevent biased inferences towards wide or unlikely distributions for the crown node of the ingroup (only *Diabelia* species) due to the uncertainty in the root area of the outgroup, we pruned the five outgroups for our ancestral state reconstructions. Three areas were defined to cover the present distribution range of *Diabelia*: (A) Japan, (B) Korea, and (C) China. Distribution areas of all populations in this study were defined according to field observations (Table S1). The BBM analyses ran for 500,000,000 generations using 10 MCMC chains.

2.8 Data accessibility

Raw Illumina data from target capture are available in the Sequence Read Archive (SRA) under accession SUB10211626 (see Table S1 for individual sample SRA accession numbers). DNA alignments, phylogenetic trees and results from all analyses and data sets can be found in the Dryad data repository XXXXXX.

3 Results

3.1 Exon assembly

The number of assembled exons per species (with > 75% of the target length; except the outgroups) ranged from 587 (*D. serrata* E314) to 989 (*D. sanguinea* E301), with an average of 889 exons per sample (Table S2; Fig. S1). The number of exons with paralog warnings (except the outgroups) ranged from 34 in *D. serrata* E314 to 619 in *D. sanguinea* E301 (Table S2). The concatenated alignment had a length of 392,600 bp, including 18,057 parsimony-informative sites, and a matrix occupancy of

bioRxiv preprint doi: https://doi.org/10.1101/2021.05.31.446416; this version posted October 26, 2021. The copyright holder for this preprint (which was not certified by peer review) is the author/funder, who has granted bioRxiv a license to display the preprint in perpetuity. It is made available under a CC-BY-ND 4.0 International license.

86.7% (Table 1). The plastid alignment resulted in a matrix of 159,365 bp with 4,693 parsimony-informative sites and a matrix occupancy of 98.2% (Table 1).

3.2 Phylogenetic reconstruction

Our nuclear phylogenetic analyses recovered the monophyly of *Diabelia* with maximum support (BS = 100; LPP = 1) and recognized five main clades: *D. serrata*, *D. stenophylla* var. *tetrasepala*, *D. sanguinea*, *D. stenophylla* and *D. spathulata*. However, the relationships of the five main groups within *Diabelia* varied among analyses and data sets.

With respect to the nuclear concatenated ML tree, the phylogeny was recovered with moderate (50 < BS ⩽ 70) to high (BS > 70) support along the five main clades (Figs. 2, S3 - S4). The monophyly of *Diabelia* was supported by 313 gene trees (out of 439 informative gene trees; ICA = 0.41) and full QS support (1.0/–/1.0; i.e., all sampled quartets supported that node). *Diabelia serrata* forms a clade with strong QS support (0.91/0.4/1) and only 34 concordant trees (out of 427; ICA = 0.02). The monophyly of *D. stenophylla* var. *tetrasepala* was supported by 158 out of 316 informative trees (ICA = 0.24) and full QS support. The sister relationship of *D. stenophylla* var. *tetrasepala* and *D. serrata* was supported by only 12 gene trees (out of 478; ICA = 0.01) and had moderate QS support with a signal of a possible alternative topology (0.21/0.35/0.99). *Diabelia sanguinea* was supported by only 24 gene trees (out of 395; ICA = 0.03) but had full QS support. The sister relationship of *D. sanguinea* and the clade of *D. serrata* + *D. stenophylla* var. *tetrasepala* was supported by only 4 gene trees (out of 490; ICA = -0.02) and moderate QS support, with a signal for a possible alternative topology (0.21/0.49/0.99). The clade of *D. stenophylla* had 43 concordant trees (out of 376; ICA =0.04) and high QS support (0.91/0.33/1). *Diabelia spathulata* was supported by 26 gene trees (out of 304; ICA = 0.06) and moderate QS support (0.22/0.29/0.98), with the sister relationship to the remainder of *Diabelia*.

The ASTRAL species tree (Fig. 3, S2) presented a largely congruent topology compared to the nuclear ML tree with all five major groupings recovered, each being respectively monophyletic. The main clades were highly supported (LPP ≥ 0.93)

bioRxiv preprint doi: https://doi.org/10.1101/2021.05.31.446416; this version posted October 26, 2021. The copyright holder for this preprint (which was not certified by peer review) is the author/funder, who has granted bioRxiv a license to display the preprint in perpetuity. It is made available under a CC-BY-ND 4.0 International license.

290 except for the sister node of *D. sanguinea* and *D. serrata* (LPP = 0.44). The
291 monophyly of *D. serrata* had strong QS support with a signal for a possible alternative
292 topology (0.92/0.38/1). *Diabelia spathulata* var. *sanguinea* was supported by moderate
293 QS support (0.62/0.78/0.99). The sister relationship of the clade of *D. sanguinea* and *D.*
294 *serrata* was supported by only four gene trees (out of 496; ICA = - 0.02) and had
295 counter QS support with signal for a possible alternative topology (-0.22/0.21/0.99).
296 *Diabelia stenophylla* var. *tetrasepala* was sister to the clade of *D. serrata* + *D.*
297 *sanguinea* with moderate QS support (0.2/0.35/0.99). The clade of *D. stenophylla*
298 between China and Japan had strong QS support (0.9/0.2/1).
299 The phylogenetic relationships in the plastid ML tree of *Diabelia* (Fig. 2 and S5)
300 were also confirmed with full QS support. The clade of *D. sanguinea* + *D. stenophylla*
301 (Japan) was sister to the *D. serrata* + *D. stenophylla* var. *tetrasepala* clade, and the
302 combined clade had strong support (BS = 98) and moderate QS score (0.14/0.57/0.98).
303 There were some observed topological differences between the plastid and nuclear
304 trees. For example, the plastid trees showed that *D. stenophylla* var. *tetrasepala* was
305 nested within *D. serrata* with strong support (BS = 98) and full QS support; *D.*
306 *sanguinea* was not-monophyletic; and *D. stenophylla* from Zhejiang was *s*ister to the
307 remainder of *Diabelia*, rather than to *D. spathulata*.
308
309 **3.3 Species network analysis**
310 The species network analyses (15-taxa data set) recovered topologies with one to
311 five reticulation events, which appear to be a better model than a strictly bifurcating
312 tree (Table 2; Fig. S6). Model selection preferred the network with two reticulation
313 events (Fig. 4). With this preferred network, the first reticulation event involved *D.*
314 *serrata* and *D. spathulata*. The inheritance probabilities of this event showed that the
315 ancestral lineage of *D. stenophylla* var. *tetrasepala* had the largest genomic
316 contribution of 65.9 % from the clade of *D. spathulata*, and a smaller portion (34.1 %)
317 came from the *D. serrata* clade. Another reticulation event was observed indicating the
318 clade of *D. spathulata* + *D. stenophylla* had genetic contributions (79.3%) from the
319 lineage leading to *D. sanguinea.*

bioRxiv preprint doi: https://doi.org/10.1101/2021.05.31.446416; this version posted October 26, 2021. The copyright holder for this preprint (which was not certified by peer review) is the author/funder, who has granted bioRxiv a license to display the preprint in perpetuity. It is made available under a CC-BY-ND 4.0 International license.

3.4 Divergence time estimation

Our dating estimates based on the nuclear data suggested an early Miocene crown age for *Diabelia* of 22.53 Ma (95% Highest Posterior Density (HPD): 17.89 - 27.73 Ma, node 1 in Fig. 5). The sister relationships of *D. serrata* and *D. stenophylla* var. *tetrasepala* diverged during the early Miocene 18.17 Ma (95% HPD: 14.07 - 22.41 Ma, node 4 in Fig. 5). The crown age of *D. serrata* was dated to 14.88 Ma (95% HPD: 11.10 - 18.91 Ma, node 5 in Fig. 5). The split between *D. spathulata* (E271) and *D. sanguinea* occurred between 3.90 and 9.41 Ma (node 7 in Fig. 5). The diversification of *D. spathulata* between Korea and Japan was estimated as 4.78 Ma (95% HPD: 3.02 - 6.84 Ma, node 8 in Fig. 5). The divergence time of *D. stenophylla* between China and Japan was 6.30 Ma (95% HPD: 3.90 - 9.41 Ma, node 6 in Fig. 5).

3.5 Ancestral area reconstruction

The reconstruction results of the ancestral distribution of *Diabelia* were presented in Fig. 6. There were three dispersal events and three vicariance events identified within the three defined biogeographic areas (Fig. 6). Our analyses revealed that the ancestor of *Diabelia* was present throughout Japan (region A) in the early Miocene (Fig. 6), followed by dispersal or vicariance events across Japan, Korea, and China. Migration events occurred primarily during the Neogene. *Diabelia spathulata* from Korea was suggested to have originated in Northeast Japan. However, one vicariance and one dispersal event were detected for the ancestral nodes of *D. stenophylla* from China, supporting their origin from Japan.

4 Discussion

4.1 Phylogenetic incongruence and hybridization, and implications for species delimitation

Our phylogenetic analyses retrieved the same five main clades of *Diabelia* in the nuclear ML tree, which are also supported in the ASTRAL tree, but the relationships

bioRxiv preprint doi: https://doi.org/10.1101/2021.05.31.446416; this version posted October 26, 2021. The copyright holder for this preprint (which was not certified by peer review) is the author/funder, who has granted bioRxiv a license to display the preprint in perpetuity. It is made available under a CC-BY-ND 4.0 International license.

among these clades are incongruent between the nuclear and plastid data (Figs. 2 and 3). For example, *D. serrata* and *D. stenophylla* var. *tetrasepala* were recovered as monophyletic in the nuclear ML tree, while *D. stenophylla* var. *tetrasepala* was nested within *D. serrata* in the plastid ML tree (Fig. 2). We not only detected widespread cytonuclear discordance across *Diabelia* (Fig. 2), but our results also showed extensive conflict among individual gene trees and the species trees (Figs. 3 and S2). Several processes can lead to gene tree inconsistencies between closely related groups, including incomplete lineage sorting (ILS), hybridization, horizontal gene transfer, or gene duplication and loss (Morales-Briones et al., 2018; Bogarin et al., 2018; Carter et al., 2019; Stull et al., 2020; Wang et al., 2021). Ancestral polymorphisms may lead to incomplete genealogical classification, therefore phylogenetic relationships between organelle markers may fail to capture the true process of population differentiation, or inconsistencies in gene trees may reflect interspecies hybridization and cytoplasmic infiltration (Lee-Yaw et al., 2019; Wielstra & Arntzen, 2020; Tkach et al., 2020). Therefore, exploring the causes of inconsistencies in gene trees may help explain the relative influences of drift, gene flow and selection on the maintenance of organelle variation within and between groups, which is helpful for revealing the evolutionary process of inter-group relationships (Mao et al., 2020; Dufresnes et al., 2020).

Comparing the topologies between the nuclear and plastid data, we found that the topology from the nuclear gene data was more stable. The nuclear data recovered five strongly supported clades (Figs. 2 and 3), with *D. serrata* forming a stable monophyletic group that was consistent with previous studies supporting the monophyletic nature of *D. serrata* (Wang et al., 2020). *Diabelia stenophylla* and *D. spathulata* were each also recovered as monophyletic based on the nuclear data. While *D. sanguinea* was not recovered as a monophyletic group in the plastid tree (Fig. 2), the possibility exists that the non-monophyly of *D. sanguinea* is due to plastid capture events or ILS (Liu et al., 2017; Renoult et al., 2009; Wang et al., 2020). Notably, the placement of *D. sanguinea* in the nuclear data had full LPP support with low ICA value and moderate QS score, which suggests that ILS and/or unidentified hybrid lineages continue to obscure our understanding of the relationship of *D. sanguinea*

bioRxiv preprint doi: https://doi.org/10.1101/2021.05.31.446416; this version posted October 26, 2021. The copyright holder for this preprint (which was not certified by peer review) is the author/funder, who has granted bioRxiv a license to display the preprint in perpetuity. It is made available under a CC-BY-ND 4.0 International license.

380 within the genus, and even the relationships of *Diabelia* as a whole, due to strong
381 signals of gene tree discordance. Previous phylogenetic relationships of *Diabelia* based
382 on only plastid data have also been unstable (Zhao et al., 2019; Wang et al., 2020). In
383 the present study, the nuclear data provide a more robust estimate of the species tree
384 compared to plastid data, suggesting that sufficiently informative molecular data are
385 important to our understanding of relationships in *Diabelia*.

386 A previous study (Zhao et al., 2019) reported gene introgression events between
387 *Diabelia* species and speculated that *D. stenophylla* var. *tetrasepala* (four big and one
388 small sepals) may have resulted from hybridization between *D. serrata* (two sepals)
389 and *D. spathulata* (five sepals). However, this hypothesis has not been confirmed. In
390 this study, we conducted network analyses for *Diabelia* and our results support the
391 existence of reticulation events within the genus (Fig. 4). Concerning the reticulate
392 evolution of the *D. stenophylla* var. *tetrasepala* clade, the inheritance contributions
393 (34.1 % and 65.9 %) support the hybridization event between *D. serrata* and *D.*
394 *spathulata.* Based on two similar morphologies but different origins of taxa within
395 *Melastoma*, Zou et al. (2017) suggested that it is difficult to infer the origins of hybrid
396 taxa based only on morphology, and the hybrids may be the result of small range
397 overlaps among parental species. Morales-Briones et al. (2018), based on the extensive
398 history of hybridization and network results in *Lachemilla*, showed the potential of
399 phylogenetic species network methods to investigate phylogenetic discordance caused
400 by ILS and hybridization. Given our network results and the distribution of *D.*
401 *stenophylla* var. *tetrasepala* partly overlaps with those of parental populations, we
402 argue that *D. stenophylla* var. *tetrasepala* may be of hybrid origin between *D. serrata*
403 and *D. spathulata*. As noted by Morales-Briones et al. (2018), additional biological
404 information is necessary for a robust interpretation of values from the phylogenetic
405 networks. Hence, we will include more samples to obtain a more robust inference of
406 relationships for future studies.

407 Despite the strong signals of gene tree discordance, our nuclear and plastid
408 phylogenies strongly supported five major clades in *Diabelia*: *Diabelia serrata*, *D.*
409 *stenophylla* var. *tetrasepala*, *D. spathulata*, *D. sanguinea*, and *D. stenophylla* (Figs. 2, 3).

bioRxiv preprint doi: https://doi.org/10.1101/2021.05.31.446416; this version posted October 26, 2021. The copyright holder for this preprint (which was not certified by peer review) is the author/funder, who has granted bioRxiv a license to display the preprint in perpetuity. It is made available under a CC-BY-ND 4.0 International license.

Especially in the nuclear data, all five major branches are monophyletic. These correspond to the species of *D. serrata*, *D. spathulata*, *D. sanguinea*, and *D. stenophylla*, but the clade of *D. stenophylla* var. *tetrasepala* does not form a monophyletic lineage with *D. stenophylla*. To resolve the non-monophyly of *D. stenophylla*, and to clarify the phylogenetic relationship within *Diabelia*, we raise *D. stenophylla* var. *tetrasepala* to the species level, recognizing it as *Diabelia tetrasepala* (Hara, 1983; Landrein, 2010). Hara (1983) also recognized *Diabelia tetrasepala* as a distinct species. Additionally, this taxon can be easily distinguished by the form of sepals (sepals 4 plus a reduced adaxial sepal lobe in *D. tetrasepala*, sepals 5 of similar size in *D. stenophylla*) (Zhao et al., 2019; Landrein and Farjon, 2020; Wang et al., 2020). Overall, based on our phylogenetic inferences (nuclear), we recognize five species in the genus (i.e., *D. serrata*, *D. tetrasepala*, *D. spathulata*, *D. sanguinea*, and *D. stenophylla*).

4.2 Molecular dating and demographic analyses

Based on our nuclear chronogram (Fig. 5), all major *Diabelia* lineages differentiated 22.53-18.17 Ma (Fig. 5). Notably, this point estimate broadly coincides with the isolation of the Japanese island (24-22 Ma) (Hotta, 1974; Iijima and Tada, 1990; Li et al., 1996; Maekawa, 1998) and the estimated dates are earlier than previous estimates based on chloroplast data (Wang et al., 2020). The East China Sea (ESC) land bridge likely acted as a barrier to the dispersal of plant species during the LGM and earlier cold periods, despite its repeated exposure during the Miocene (7.0-5.0 Ma) and Quaternary (2.0-1.3 Ma, 0.2-0.015 Ma) (Harrison, 2001). Even though the Japanese archipelago was not covered by a major ice sheet during the last glacial period (Ono, 1984), the mean annual temperature was 5℃-9℃ cooler and the precipitation was less than at present (Yasuda and Narita, 1981; Tsukada, 1988). In addition, because of lower sea levels (ca. 100 m below present), Shikoku and Kyushu were continuous with Honshu, and the continental shelf, ca. 20-30 km from the present coastline, emerged around the archipelago (Ohta and Yonekura, 1987). The distribution data of *D. serrata* suggests a wide distribution in Japan except for Hokkaido. As the climate warmed, the species recovered and expanded northward or towards higher

bioRxiv preprint doi: https://doi.org/10.1101/2021.05.31.446416; this version posted October 26, 2021. The copyright holder for this preprint (which was not certified by peer review) is the author/funder, who has granted bioRxiv a license to display the preprint in perpetuity. It is made available under a CC-BY-ND 4.0 International license.

altitudes (Tsukada, 1988; Takahara et al., 2000), therefore, forming the current isolated distribution.

Diabelia species are relatively tolerant to cold and arid climates, which might have facilitated gene exchange across the glacially exposed ECS land bridge up until its latest submergence. All *Diabelia* species have fruits forming samaras, which increase long-distance dispersal abilities (Landrein, 2010). Our molecular dating indicates that *Diabelia* originated in the Japanese archipelago (Fig. 5) and the onset of diversification of *D. stenophylla* from Japan and *D. stenophylla* from China occurred during the early Pliocene. Our results suggest a vicariance event and a dispersal event associated with *D. stenophylla* from China (Fig. 6). Under the hypothesis of long-distance dispersal, a predicted lineage in one region should nest within a lineage from a separate disjunctive region. In contrast, under vicariance, lineages from different geographic regions would each be monophyletic with relatively comparable levels of genetic diversity in each region of the distribution (Yoder & Nowak, 2006; Liao et al., 2016; Thomas et al., 2017). The disjunction between *D. stenophylla* in Japan and *D. stenophylla* from China may have resulted from migration across this land bridge followed by vicariance.

Our results show that that the interchanges of the populations of *D. spathulata* between Korea and Japan are frequent. The close relationships between Japan and Korea have also been observed in other taxa such as *Meehania urticifolia* (Takano et al., 2020) and *Kirengeshoma koreana* (Qiu et a1., 2011). Furthermore, our results also suggest that populations of *D. spathulata* in Korea originated from Japan and are likely due to recent vicariance and dispersal events (Fig. 6), which is largely congruent with the previous conclusions by Wang et al. (2020). Wang et al. (2020) showed that the populations between Korea and the northern Japan may have resulted from a vicariance event. Our results further suggest an early and a later dispersal event, supporting a highly dynamic biogeographic relationships between Japan and Korea. Our divergence time estimates suggest that species differentiation in *D. spathulata* occurred during the late Miocene to the early Pliocene (4.78 Ma, 95% HPD: 3.02 – 6.84 Ma), suggesting that extant populations likely differentiated well before the LGM.

bioRxiv preprint doi: https://doi.org/10.1101/2021.05.31.446416; this version posted October 26, 2021. The copyright holder for this preprint (which was not certified by peer review) is the author/funder, who has granted bioRxiv a license to display the preprint in perpetuity. It is made available under a CC-BY-ND 4.0 International license.

The cooling and drying climate in the late Miocene drove the formation of *D. spathulata*. The changing climate in the late Pliocene and Pleistocene is related to lineage differentiation, genetic diversity, and population contraction and expansion, which have also been observed in *Cercidiphyllum japonicum* (Qi et al., 2012) and *Euptelea* (Cao et al., 2016). This study adds another example of this well-documented pattern.

5 Conclusions

A robust phylogeny of *Diabelia* was reconstructed with nuclear and plastid data based on target enrichment and genome skimming approaches. The inferred phylogenies from both nuclear and plastome data indicate that *Diabelia* can be divided into five main clades, which are further supported by morphological traits such as number of sepals, nectary cushion position, and corolla color. Our results show clear cytonuclear discordance and strong conflict between individual gene trees and species trees in *Diabelia*. The PhyloNet results further confirmed the existence of reticulation events in *Diabelia*, supporting that *D. tetrasepala* was the result of a hybridization event. The divergence time and biogeographic analyses further support the differentiation and propagation of *Diabelia* with multiple vicariance events from the perspective of time and space, further supporting the complex natural hybridization and evolutionary network of the disjunctive flora of Japan and China. Tree-like and reticulate evolution should be considered when reconstructing phylogenetic relationships among closely related species. The appropriate choice of data to construct phylogenetic trees is important in the era of genomics. Further studies are needed to clarify the origin, dispersal and evolution of Sino-Japanese disjunct species with nuclear and plastid data at the population level. Finally, our results shed light on the species delimitation, supporting the recognition of five species in *Diabelia*, corresponding to the five main clades within the genus in the nuclear phylogeny.

Taxonomic treatment

Based on our results, we formally recognize five species in *Diabelia*. Landrein &

bioRxiv preprint doi: https://doi.org/10.1101/2021.05.31.446416; this version posted October 26, 2021. The copyright holder for this preprint (which was not certified by peer review) is the author/funder, who has granted bioRxiv a license to display the preprint in perpetuity. It is made available under a CC-BY-ND 4.0 International license.

Farjon (2019) treated four of the five species, i.e., *D. sanguinea*, *D. serrata*, *D. stenophylla*, and *D. spathulata*. Below we provide the synoptic treatment for *Diabelia tetrasepala*.

Diabelia tetrasepala (Koidz.) Landrein, Phytotaxa 3: 37. 2010.

Basionym: *Abelia spathulata* Siebold & Zucc. var. *tetrasepala* Koidz., Bot. Mag. (Tokyo) 29 (348): 311. 1915.

Abelia tetrasepala (Koidz.) H. Hara & S. Kuros. in Kurosawa & Hara, J. Jap. Bot. 30: 296. 1955; *Diabelia stenophylla* (Honda) Landrein var. *tetrasepala* (Koidz.) Landrein, Kew Bull. 74(4)-70: 186. 2019.

Abelia spathulata Siebold & Zucc. var. *subtetrasepala* Makino, J. Jap. Bot. 1: 18. 1917.

Abelia spathulata Siebold & Zucc. var. *subtetrasepala* Makino f. *flavescens* Honda, J. Jap. Bot. 11: 569. 1935.

Acknowledgements

The work was funded by Hainan Provincial Natural Science Foundation of China (421RC486) and National Natural Science Foundation of China (31660055). We thank Gabriel Johnson for his help with the target enrichment experiment, and the United States National Herbarium for permission to sample some collections. We acknowledge the staff in the Laboratories of Analytical Biology at the National Museum of Natural History, the Smithsonian Institution for support and assistance.

Author contributions

H.-F.W. and J.W. conceived the study. H.-F.W. and D.F.M-B. performed the research and analyzed the data. X.-R.K., H.-F.W., D.F.M-B., J.W., H.-X.W., Q.-H.S. and J.B.L. wrote and revised the manuscript.

bioRxiv preprint doi: https://doi.org/10.1101/2021.05.31.446416; this version posted October 26, 2021. The copyright holder for this preprint (which was not certified by peer review) is the author/funder, who has granted bioRxiv a license to display the preprint in perpetuity. It is made available under a CC-BY-ND 4.0 International license.

References

Akaike, H. 1973. Information theory and an extension of the maximum likelihood principle. In: Petrov BN, Csaki F, eds. Second international symposium on information theory. Budapest, Hungary: Akademiai Kiado, 267-281.

Banfer, G., Moog, U., Fiala, B., Mohamed, M., Weising, K., Blattner, F.R. 2006. A chloroplast genealogy of myrmecophytic Macaranga species (Euphorbiaceae) in Southeast Asia reveals hybridization, vicariance and long-distance dispersals. *Molecular Ecology* 15: 4409-4424.

Bell CD, Donoghue MJ. 2005. Dating the Dipsacales: comparing models, genes, and evolutionary implications. *American Journal of Botany* 92: 284-296.

Bobo-Pinilla J, de Giles JP, López-González N, Mediavilla S, Martínez-Ortega MM. 2018. Phylogeography of an endangered disjunct herb: long-distance dispersal, refugia and colonization routes. *AoB PLANTS* 10: ply047.

Bogarin D, Pérez-Escobar OA, Groenenberg D, Holland SD, Karremans AP, Lemmon EM, Lemmon AR, Pupulin F, Smets E, Gravendeel B. 2018. Anchored Hybrid Enrichment generated nuclear, plastid and mitochondrial markers resolve the *Lepanthes horrida* (Orchidaceae: Pleurothallidinae) species complex. *Molecular Phylogenetics and Evolution* 129: 27-47.

Bolger AM, Lohse, M, Usadel B. 2014. Trimmomatic: A flexible trimmer for Illumina Sequence Data. *Bioinformatics (Oxford, England)* 30: 2114-2120.

Bouckaert R, Heled J, Kuhnert D, Vaughan T, Wu CH, Xie D, Suchard MA, Rambaut A, Drummond AJ. 2014. BEAST 2: a software platform for Bayesian evolutionary analysis. *PLoS Computational Biology* 10: e1003537.

Buys MH, Winkworth RC, De Lange PJ, Wilson PG, Mitchell N, Lemmon AR, Moriarty LE, Holland S, Cherry JR, Klápště J. 2019. The phylogenomics of diversification on an island: applying anchored hybrid enrichment to New Zealand *Leptospermum scoparium* (Myrtaceae). *Botanical Journal of the Linnean Society* 191: 1-17.

bioRxiv preprint doi: https://doi.org/10.1101/2021.05.31.446416; this version posted October 26, 2021. The copyright holder for this preprint (which was not certified by peer review) is the author/funder, who has granted bioRxiv a license to display the preprint in perpetuity. It is made available under a CC-BY-ND 4.0 International license.

Cao YN, Comes HP, Sakaguchi S, Chen LY, Qiu YX. 2016. Evolution of East Asia's Arcto-Tertiary relict *Euptelea* (Eupteleaceae) shaped by Late Neogene vicariance and Quaternary climate change. *BMC Evolutionary Biology* 16: 1.

Carter Katherine A, Liston Aaron, Bassil Nahla V, Alice Lawrence A, Bushakra Jill M, Sutherland Brittany L, Mockler Todd C, Bryant Douglas W, Hummer Kim E. 2019. Target Capture Sequencing Unravels *Rubus* Evolution. *Frontiers in Plant Science* 10: 1615.

Casebolt S, Kowalewski M. 2018. Mollusk shell assemblages as archives of spatial structuring of benthic communities around subtropical islands. *Estuarine Coastal and Shelf Science* 215: 132-143.

Doyle JA, Sauquet H, Scharaschkin T, Thomas LA. 2004. Phylogeny, molecular and fossil dating, and biogeographic history of Annonaceae and Myristicaceae (Magnoliales). *International Journal of Plant Sciences* 165: S55–S67.

Doyle JJ, Doyle J. 1987. A rapid DNA isolation procedure for small quantities of fresh leaf tissue. *Phytochemical Bulletin* 19: 11-15.

Drummond AJ, Suchard MA, Xie D, Rambaut A. 2012. Bayesian phylogenetics with BEAUti and the BEAST 1.7. *Molecular Biology Evolution* 29: 1969-1973.

Dufresnes C, Nicieza AG, Litvinchuk SN, Rodrigues N, Jeffries DL, Vences M, Perrin N, Martinez-Solano I. 2020. Are glacial refugia hotspots of speciation and cytonuclear discordances? Answers from the genomic phylogeography of Spanish common frogs. *Molecular Ecology* 29: 986-1000.

Granados Mendoza C, Jost M, Hágsater E, Magallón S, van den Berg C, Lemmon EM, Lemmon AR,Salazar GA,Wanke S. 2020. Target Nuclear and Off-Target Plastid Hybrid Enrichment Data Inform a Range of Evolutionary Depths in the Orchid Genus *Epidendrum*. *Frontiers in Plant Science* 10: 1761.

Hahn C, Bachmann L, Chevreux B. 2013. Reconstructing mitochondrial genomes directly from genomic next-generation sequencing reads-a baiting and iterative mapping approach. *Nucleic Acids Research* 41: e129.

Haq ZU, Khan SM, Ahmad Z, Abdullah, Shah SA, Mustafa G, Razzaq A, Manan F, Ullah A, Hussain M. 2020. An Evaluation of Conservation Status and Ecological

bioRxiv preprint doi: https://doi.org/10.1101/2021.05.31.446416; this version posted October 26, 2021. The copyright holder for this preprint (which was not certified by peer review) is the author/funder, who has granted bioRxiv a license to display the preprint in perpetuity. It is made available under a CC-BY-ND 4.0 International license.

Zonation of *Alnus Nitida*; A Monophyletic Species of the Sino-japanese Region. *Journal of Animal and Plant Sciences* 30: 1224-1235.

Hara H. 1983. A revision of Caprifoliaceae of Japan with reference to allied plants in other districts and the Adoxaceae. *Ginkgoana* 5: 1-336.

Harrison SP, Yu G, Takahara H, Prentice IC. 2001. Palaeovegetation: Diversity of temperate plants in East Asia. *Nature* 413: 129-130.

Hotta M. 1974. History and geography of plants. Tokyo: Sanseido.

Iijima A, Tada R. 1990. Evolution of Tertiary sedimentary basins of Japan in reference to opening of the Japan Sea. J*ournal of the Faculty of Science University of Tokyo* 2: 121-171.

Jiang XL, Deng M, Li Y. 2016. Evolutionary history of subtropical evergreen broad-leaved forest in Yunnan Plateau and adjacent areas: an insight from *Quercus schottkyana* (Fagaceae). *Tree Genetics & Genomes* 12: 104.

Ji YH, Yang LF, Chase MW, Liu CK, Yang ZY, Yang J, Yang JB, Yi TS. 2019. Plastome phylogenomics biogeography and clade diversification of *Paris* (Melanthiaceae). *BMC Plant Biology* 19: 543.

Johnson MG, Gardner EM, Liu Y, Medina R, Goffinet B, Shaw AJ, Zerega NJC, Wickett NJ. 2016. HybPiper: extracting coding sequence and introns for phylogenetics from high-throughput sequencing reads using target enrichment. *Applications in Plant Sciences* 4: 1600016.

Katoh K and Standley DM. 2013. MAFFT multiple sequence alignment software version 7: improvements in performance and usability. *Molecular Biology and Evolution* 30: 772-780.

Landrein S. 2010. *Diabelia*, a new genus of tribe Linnaeeae subtribe Linnaeinae (Caprifoliaceae). *Phytotaxa* 3: 34-38.

Landrein S, Prenner G, Chase MW, Clarkson JJ. 2012. *Abelia* and relatives, phylogenetics of Linnaeeae(Dipsacales-Caprifoliaceae s.l.) and a new interpretation of their inflorescence morphology. *Botanical Journal of the Linnean Society* 169: 692-713.

bioRxiv preprint doi: https://doi.org/10.1101/2021.05.31.446416; this version posted October 26, 2021. The copyright holder for this preprint (which was not certified by peer review) is the author/funder, who has granted bioRxiv a license to display the preprint in perpetuity. It is made available under a CC-BY-ND 4.0 International license.

Landrein S, Farjon A. 2019. A monograph of Caprifoliaceae: Linnaeeae. *Kew Bulletin* 74: 70.

Leducq JB, Henault M, Charron G, Nielly-Thibault L, Terrat Y, Fiumera HL, Shapiro BJ, Landry CR. 2017. Mitochondrial Recombination and Introgression during Speciation by Hybridization. *Molecular Biology and Evolution* 34: 1947-1959.

Lee-Yaw JA, Grassa CJ, Joly S, Andrew RL,Rieseberg LH. 2019. An evaluation of alternative explanations for widespread cytonuclear discordance in annual sunflowers (*Helianthus*). *New Phytologist* 221: 515-526.

Li SF, Chang ZY, Yuan YM. 1996. The origin and dispersal of the genus *Clintonia* Raf. (Liliaceae): Evidence from its cytogeography and morphology. *Caryologia* 49: 125-135.

Liao YY, Gichira AW, Wang QF, Chen JM. 2016. Molecular phylogeography of four endemic *Sagittaria* species (Alismataceae) in the Sino-Japanese Floristic Region of East Asia. *Botanical Journal of the Linnean Society* 180: 6-20.

Liu X, Wang ZS, Shao WH, Ye ZY, Zhang JG. 2017. Phylogenetic and Taxonomic Status Analyses of the Abaso Section from Multiple Nuclear Genes and Plastid Fragments Reveal New Insights into the North America Origin of *Populus* (Salicaceae). Frontiers in Plant Science 7: doi: 10.3389/fpls.2016.02022.

Lu RS, Chen Y, Tamaki I, Sakaguchi S, Ding YQ, Takahashi D, Li P, Isaji Y, Chen J, Qiu YX. 2020. Pre-quaternary diversification and glacial demographic expansions of *Cardiocrinum* (Liliaceae) in temperate forest biomes of Sino-Japanese Floristic Region. *Molecular Phylogenetics and Evolution* 143: 106693.

Maekawa F. 1998. The origin of plants (Syokubutsuno-kitamichi). Tokyo: Yasaka-Syobou.

Maddison WP, Maddison DR, 2018. Mesquite: a modular system for evolutionary analysis. Version 3, 6. http://www.mesquiteproject.org.

Maguilla E, Escudero M, Ruiz-Martin J, Arroyo J. 2021. Origin and diversification of flax and their relationship with heterostyly across the range. *Journal of Biogeography* 48: 1994-2007.

bioRxiv preprint doi: https://doi.org/10.1101/2021.05.31.446416; this version posted October 26, 2021. The copyright holder for this preprint (which was not certified by peer review) is the author/funder, who has granted bioRxiv a license to display the preprint in perpetuity. It is made available under a CC-BY-ND 4.0 International license.

Mao XG, Rossiter SJ. 2020. Genome-wide data reveal discordant mitonuclear introgression in the intermediate horseshoe bat (*Rhinolophus affinis*). *Molecular phylogenetics and evolution* 150: 106886.

Martínez-Espinosa C, Sauvage S, Al Bitar A, Green PA, Vörösmarty CJ, Sánchez-Pérez JM. 2021. Denitrification in wetlands: A review towards a quantification at global scale. *Science of the total environment* 754: 142398.

Miller MA, Pfeiffer W, Schwartz T. 2010. Creating the CIPRES Science Gateway for inference of large phylogenetic trees. *Gateway Computing Environments Workshop* 1-8.

Mitsui Y, Chen ST, Zhou ZK, Peng CI, Deng YF, Setoguchi H. 2008. Phylogeny and biogeography of the genus *Ainsliaea* (Asteraceae) in the Sino-Japanese region based on nuclear rDNA and plastid DNA sequence data. *Annals of Botany* 101: 111-124.

Morales-Briones DF, Liston A, Tank DC. 2018. Phylogenomic analyses reveal a deep history of hybridization and polyploidy in the Neotropical genus *Lachemilla* (Rosaceae). *New Phytologist* 218: 1668-1684.

Morales-Briones DF, Gehrke B, Huang CX, Liston A, Ma H, Marx HE, Tank DC, Yang Y. 2021. Analysis of paralogs in target enrichment data pinpoints multiple ancient polyploidy events in *Alchemilla* s.l. (Rosaceae). *Systematic Biology* 10.1093/sysbio/syab032.

Nge FJ, Kellermann J, Biffin E, Waycott M, Thiele KR. 2021. Historical biogeography of *Pomaderris* (Rhamnaceae): Continental vicariance in Australia and repeated independent dispersals to New Zealand. *Molecular Phylogenetics and Evolution* 158: 107085.

Nguyen LT, Schmidt HA, von Haeseler A, Minh, BQ. 2015. IQ-TREE: a fast effective stochastic algorithm for estimating maximum-likelihood phylogenies. *Molecular Biology and Evolution* 32: 268-274.

Ohta Y, Yonekura N. 1987. Coastal line. In Japan Association for Quaternary Research [ed.], Quaternary Maps of Japan, 70-72. University of Tokyo Press, Tokyo, Japan (in Japanese).

bioRxiv preprint doi: https://doi.org/10.1101/2021.05.31.446416; this version posted October 26, 2021. The copyright holder for this preprint (which was not certified by peer review) is the author/funder, who has granted bioRxiv a license to display the preprint in perpetuity. It is made available under a CC-BY-ND 4.0 International license.

Ono Y. 1984. Late glacial paleoclimate reconstructed from glacial and periglacial landforms in Japan. *Geographical Review of Japan, Series B* 57:80-100 (in Japanese).

Ota H. 1998. Geographic patterns of endemism and speciation in amphibians and reptiles of the Ryukyu Archipelago, Japan, with special reference to their paleogeographical implications. *Population Ecology* 40: 189-204.

Pease JB, Brown JW, Walker JF, Hinchliff CE, Smith SA. 2018. Quartet Sampling distinguishes lack of support from conflicting support in the green plant tree of life. *American Journal of Botany* 105: 385-403.

Qi XS, Chen C, Hans PC, Sakaguchi S, Liu YH, Tanaka N, Sakio H, Qiu YX. 2012. Molecular data and ecological niche modelling reveal a highly dynamic evolutionary history of the East Asian Tertiary relict *Cercidiphyllum* (Cercidiphyllaceae). *New Phytologist* 196: 617-630.

Qiu YX, Guan BC, Fu CX, Comes HP. 2009. Did glacials and/or interglacials promote allopatric incipient speciation in East Asian temperate plants? Phylogeographic and coalescent analyses on refugial isolation and divergence in *Dysosma versipellis*. *Molecular Phylogenetics and Evolution* 51: 281-293.

Qiu YX, Fu CX, Comes HP. 2011. Plant molecular phylogeography in China and adjacent regions: Tracing the genetic imprints of Quaternary climate and environmental change in the world's most diverse temperate flora. M*olecular Phylogenetics and Evolution* 59: 225-244.

Renoult JP, Kjellberg F, Grout C, Santoni S, Khadari B. 2009. Cyto-nuclear discordance in the phylogeny of *Ficus* section *Galoglychia* and host shifts in plant-pollinator associations. *BMC Evolutionary Biology* 9: 248.

Salichos L, Stamatakis A, Rokas A. 2014. Novel information theory-based measures for quantifying incongruence among phylogenetic trees. *Molecular Biology and Evolution* 31: 1261-1271.

Sayyari E, Mirarab S. 2016. Fast coalescent-based computation of local branch support from quartet frequencies. *Molecular Biology and Evolution* 33: 1654-1668.

Schneider JV, Jungcurt T, Cardoso D, Amorim AM, Töpel M, Andermann T, Poncy O,

bioRxiv preprint doi: https://doi.org/10.1101/2021.05.31.446416; this version posted October 26, 2021. The copyright holder for this preprint (which was not certified by peer review) is the author/funder, who has granted bioRxiv a license to display the preprint in perpetuity. It is made available under a CC-BY-ND 4.0 International license.

Berberich T, Zizka G. 2020. Phylogenomics of the tropical plant family Ochnaceae using targeted enrichment of nuclear genes and 250+ taxa. *TAXON* 70: 48-71.

Schwarz G. 1978. Estimating the dimension of a model. *Annals of Statistics* 6: 461-464.

Shin HT, Yi MH, Shin JS, Lee BC, Yoon JW. 2012. Distribution of rare plants-Ulsan, Busan, Yangsan. *Journal of Korean Nature* 5: 145-153.

Smith SA, Dunn CW. 2008. Phyutility: a phyloinformatics tool for trees, alignments and molecular data. *Bioinformatics* 24: 715-716.

Smith SA, Moore MJ, Brown JW, Yang Y. 2015. Analysis ofcphylogenomic datasets reveals conflict, concordance, and genecduplications with examples from animals and plants. *BMC Evolutionary Biology* 15: 150.

Stamatakis A. 2014. RAxML version 8: a tool for phylogenetic analysis and post analysis of large phylogenies. *Bioinformatics* 30: 1312-1313.

Stull GW, Soltis PS, Soltis DE, Gitzendanner MA, Smith SA. 2020. Nuclear phylogenomic analyses of asterids conflict with plastome trees and support novel relationships among major lineages. *American Journal of Botany* 107: 790-805.

Sugiura N. 1978. Further Analysis of the Data by Akaike's Information Criterion and the Finite Corrections. *Communications in Statistics-Theory and Methods A* 7: 13-26.

Takahara H, Sugita S, Harrison SP, Miyoshi N, Morita Y, Uchiyama T. 2000. Pollen-based reconstructions of Japanese biomes at 0,6000 and 18,000 14C yr BP. *Journal of Biogeography* 27: 665-683.

Takano A, Sakaguchi S, Li P, Matsuo A, Suyama Y, Xia GH, Liu X, Isagi Y. 2020. A Narrow Endemic or a Species Showing Disjunct Distribution? Studies on *Meehania montis-koyae* Ohwi (Lamiaceae). *Plants* 9: 1159.

Thomas DC, Tang CC, Saunders RMK. 2017. Historical biogeography of *Goniothalamus* and Annonaceae tribe Annoneae: dispersal-vicariance patterns in tropical Asia and intercontinental tropical disjunctions revisited. *Journal of Biogeography* 44: 2862-2876.

bioRxiv preprint doi: https://doi.org/10.1101/2021.05.31.446416; this version posted October 26, 2021. The copyright holder for this preprint (which was not certified by peer review) is the author/funder, who has granted bioRxiv a license to display the preprint in perpetuity. It is made available under a CC-BY-ND 4.0 International license.

Tian B, Fu Y, Milne RI, Mao KS, Sun YS, Ma XG, Sun H. 2020. A complex pattern of post-divergence expansion, contraction, introgression, and asynchronous responses to Pleistocene climate changes in two *Dipelta* sister species from western China. *Journal of Systematics and Evolution* 58: 247-262.

Tkach N, Schneider J, Doering E, Woelk A, Hochbach A, Nissen J, Winterfeld G, Meyer S, Gabriel J, Hoffmann MH, Roeser M. 2020. Phylogenetic lineages and the role of hybridization as driving force of evolution in grass supertribe Poodae. *TAXON* 69: 234-277.

Toews DPL, Brelsford A. 2012. The biogeography of mitochondrial and nuclear discordance in animals. *Molecular Ecology* 21: 3907-3930.

Torres-Cambas Y, Ferreira S, Cordero-Rivera A, Lorenzo-Carballa MO. 2019. Mechanisms of allopatric speciation in an Antillean damselfly genus (Odonata, Zygoptera): Vicariance or long-distance dispersal? *Molecular Phylogenetics and Evolution* 137: 14-21.

Tsukada M. 1988. Japan. In B. Huntley and T. Webb III [eds.], Vegetation history, 459-518. Kluwer Academic, Dordrecht, Netherlands.

Wang HF，Landrein S，Dong WP，Nie ZL, Kondo K, Funamoto T, Wen J, Zhou SL. 2015. Molecular phylogeny and biogeographic diversification of linnaeoideae (Caprifoliaceae s. l.) disjunctly distributed in Eurasia, North America and Mexico. *PLoS ONE* 10: 1-26.

Wang HX, Moore MJ, Barrett RL, Landrein S, Sakaguchi S, Maki M, Wen J and Wang HF. 2020. Plastome phylogenomic insights into the Sino-Japanese biogeography of *Diabelia* (Caprifoliaceae). *Journal of Systematics and Evolution* 58: 972-987.

Wang HX, Morales-Briones FD, Moore MJ, Wen J, Wang HF. 2021. A phylogenomic perspective on gene tree conflict and character evolution in Caprifoliaceae using target enrichment data, with Zabelioideae recognized as a new subfamily. *Journal of Systematics and Evolution* 59: 897-914.

Wang JF, Gong X, Chiang YC, Kuroda C. 2013. Phylogenetic patterns and disjunct distribution in *Ligularia hodgsonii* Hook. (Asteraceae). *Journal of Biogeography* 40: 1741-1754.

bioRxiv preprint doi: https://doi.org/10.1101/2021.05.31.446416; this version posted October 26, 2021. The copyright holder for this preprint (which was not certified by peer review) is the author/funder, who has granted bioRxiv a license to display the preprint in perpetuity. It is made available under a CC-BY-ND 4.0 International license.

Wang PC, Yao HY, Kadeem JG, Lu Q, Hao Y, Zhang ZW, Wang N. 2018. Glaciation-based isolation contributed to speciation in a Palearctic alpine biodiversity hotspot: evidence from endemic species. *Molecular Phylogenetics and Evolution* 129: 315-324.

Wanke S, Granados MC, Müller S, Paizanni GA, Neinhuis C, Lemmon AR, Lemmon EM, Samain MS. 2017. Recalcitrant deep and shallow nodes in *Aristolochia* (Aristolochiaceae) illuminated using anchored hybrid enrichment. *Molecular Phylogenetics and Evolution* 117: 111-123.

Weitemier K, Straub SCK, Cronn RC, Fishbein M, Schmickl R, McDonnell A, Liston A. 2014. Hyb-Seq: combining target enrichment and genome skimming for plant phylogenomics. *Applications in Plant Sciences* 2: 9.

Wen D, Yu Y, Zhu J, Nakhleh L. 2018. Inferring phylogenetic networks using PhyloNet. *Systematic Biology* 67: 735-740.

Wielstra B, Arntzen JW. 2020. Extensive cytonuclear discordance in a crested newt from the Balkan Peninsula glacial refugium. *Biological Journal of the Linnean Society* 130: 578-585.

Yao X, Tan YH, Yang JB, Wang Y, Corlett RT, Manen JF. 2019. Exceptionally highrates of positive selection on the rbcL gene in the genus *Ilex* (Aquifoliaceae). *BMC Evolutionary Biology* 19: 129.

Yasuda Y, Narita K. 1981. Calculated thermal index maps for the reconstruction of past vegetation since the last glacial age in Japan. *Geographical Review of Japan* 54: 369-381.

Yang QE, Landrein S, Osborne J, Borosova R. 2011. Caprifoliaceae. Flora of China. Science Press, Beijing, and Missouri Botanical Garden Press, St. Louis. 19: 616-641.

Yang Y, Smith SA. 2014. Orthology inference in nonmodel organisms using transcriptomes and low-coverage genomes: Improving accuracy and matrix occupancy for phylogenomics. *Molecular Biology and Evolution* 31: 3081-3092.

bioRxiv preprint doi: https://doi.org/10.1101/2021.05.31.446416; this version posted October 26, 2021. The copyright holder for this preprint (which was not certified by peer review) is the author/funder, who has granted bioRxiv a license to display the preprint in perpetuity. It is made available under a CC-BY-ND 4.0 International license.

Yoder AD, Nowak MD. 2006. Has vicariance or dispersal been the predominant biogeographic force in Madagascar? Only time will tell. *Annual Review of Ecology, Evolution, and Systematics* 37: 405 - 431.

Yu Y, Harris AJ, Blair C, He XJ, 2015. RASP (Reconstruct Ancestral State in Phylogenies): a tool for historical biogeography. *Molecular Phylogenetics and Evolution* 87: 46-49.

Yu Y, Nakhleh L. 2015. A maximum pseudo-likelihood approach for phylogenetic networks. *BMC Genomics* 16: S10.

Zhai SN, Comes PH, Nakamura K, Yan HF, Qiu YX. 2012. Late Pleistocene lineage divergence among populations of *Neolitsea sericea* (Lauraceae) across a deep sea-barrier in the Ryukyu Islands. *Journal of Biogeography* 39: 1347-1360.

Zhang C, Rabiee M, Sayyari E, Mirarab S. 2018. ASTRAL-III: polynomial time species tree reconstruction from partially resolved gene trees. *BMC Bioinformatics*. 19: 523.

Zhang MH, Wang CY, Zhang C, Zhang DG, Li KG, Nie ZL, Meng Y. 2020. Phylogenetic relationships and biogeographic history of the unique *Saxifraga* sect. *Irregulares* (Saxifragaceae) from eastern Asia. *Journal of Systematics and Evolution* 58: 958-971.

Zhao KK, Landrein S, Barrett RL, Sakaguchi S, Maki M, Mu WX, Yang T, Zhu ZX, Liu H, Wang HF. 2019. Phylogeographic analysis and genetic structure of an endemic Sino-Japanese disjunctive genus *Diabelia* (Caprifoliaceae). *Frontiers in Plant Science* 10: 913.

Zhou SL, Funamota T, Wen J. 2004. Species relationships in *Abelia* sect. *Abelia* (Caprifoliaceae) in east Asia and verification of distribution of *A. serrata* in China, evidence from AFLP analysis. *Acta Bot Yunnan* 26: 405-412.

Zhou SL, Funamota T, Huang PH, Wen J. 2006. Discovery of *Abelia spathulate* (Caprifoliaceae) in eastern China. *Acta Phytotaxonomica Sinica* 44: 467-470.

Zou PS, Ng WL, Wu W, Dai SP, Ning ZL, Wang SQ, Liu Y, Fan Q, Zhou RC. 2017. Similar morphologies but different origins: hybrid status of two more semi-creeping taxa of *Melastoma*. *Frontiers in Plant Science* 8: 673.

bioRxiv preprint doi: https://doi.org/10.1101/2021.05.31.446416; this version posted October 26, 2021. The copyright holder for this preprint (which was not certified by peer review) is the author/funder, who has granted bioRxiv a license to display the preprint in perpetuity. It is made available under a CC-BY-ND 4.0 International license.

Figure Legends

Fig. 1. Floral diversity of *Diabelia*. (A) *Diabelia serrata* (Photograph by Difei Wu), (B) *D. serrata var. buchwaldii* (Photograph by Shota Sakaguchi), (C) *D. stenophylla* var. *tetrasepala* (Photograph by Shota Sakaguchi), (D) *D. spathulata* (Photograph by Kyoungsu Choi), (E) *D. spathulata* (Photograph by Sven Landrein), (F) *D. sanguinea* (Photograph by Sven Landrein).

Fig. 2. Tanglegram of the nuclear concatenated (left) and plastid (right) phylogenies of *Diabelia*. Dotted lines connect taxa between the two phylogenies. Maximum likelihood bootstrap support values are shown above branches. The asterisks indicate maximum likelihood bootstrap support of 100%. Major taxonomic groups or main clades in the family as currently recognized are indicated by branch colors as a visual reference to relationships.

Fig. 3. ASTRAL species tree of *Diabelia*; Clade support is depicted as: Local posterior probability (LPP)/Quartet concordance (QC)/Quartet differential (QD)/Quartet informativeness (QI).

Fig. 4. Best supported species network inferred with PhyloNet for the 15-taxa. Numbers next to the inferred hybrid branches indicate inheritance probabilities. Blue curved lines represent major hybrid edges. Red curved lines represent minor hybrid edges (edges with an inheritance contribution < add space 0.50).

Fig. 5. BEAST analysis of divergence times based on the nuclear data set. Calibration points are indicated by A, B. Numbers 1-8 represent major divergence events in *Diabelia*; mean divergence times and 95% highest posterior densities (HDP) are provided for each node of interests. Blue bars represent 95% HDP.

Fig. 6. Ancestral area reconstruction for *Diabelia*. Areas of endemism are as follows: (A) Japan, (B) Korea, (C) China. The numbered nodes represent crown nodes of important colonization events.

Table 1. Data set statistics, including the number of taxa, number of characters, number of PI characters, missing data.

Table 2. Model selection of the different species networks and bifurcating trees.

bioRxiv preprint doi: https://doi.org/10.1101/2021.05.31.446416; this version posted October 26, 2021. The copyright holder for this preprint (which was not certified by peer review) is the author/funder, who has granted bioRxiv a license to display the preprint in perpetuity. It is made available under a CC-BY-ND 4.0 International license.

Fig. S1. Heatmaps showing gene recovery efficiency for the nuclear genes in 42 species of *Diabelia*. Columns represent genes, and each row is one sample. Shading indicates the percentage of the reference locus length coverage.

Fig. S2. ASTRAL species tree. Numbers above branches indicate the number of gene trees concordant/conflicting with that node in the species tree. Numbers below the branches are the Internode Certainty All score. Pie charts next to the nodes present the proportion of gene trees that supports that clade (blue), the proportion that supports the main alternative for that clade (green), the proportion that supports the remaining alternatives (red), light gray means missing data, and dark gray means uninformative (BS < 50%).

Fig. S3. Results of the Quartet Sampling of the nuclear RAxML tree; Clade support is depicted as: Local posterior probability (LPP)/Quartet concordance (QC)/Quartet differential (QD)/Quartet informativeness (QI).

Fig. S4. Nuclear RAxML tree. Numbers above branches indicate the number of gene trees concordant/conflicting with that node in the species tree. Numbers below the branches are the Internode Certainty All score. Pie charts next to the nodes present the proportion of gene trees that supports that clade (blue), the proportion that supports the main alternative for that clade (green), the proportion that supports the remaining alternatives (red), light gray means missing data, and dark gray means uninformative (BS < 50%).

Fig. S5. Results of the Quartet Sampling of the plastid IQ-tree tree; Clade support is depicted as: Local posterior probability (LPP)/Quartet concordance (QC)/Quartet differential (QD)/Quartet informativeness (QI).

Fig. S6. Best species networks of the selective nuclear data set estimated with PhyloNet for the 15-taxa data set. A: One hybridization event; B: Two hybridization events; C: Three hybridization events; D: Four hybridization events; F: Five hybridization events. Blue branches connect the hybrid nodes. Numbers next to blue branches indicate inheritance probabilities.

Table S1. List of species and vouchers used in this study.

Table S2. HybPiper assembly statistics.

Table 1. Data set statistics, including the number of taxa, number of characters, number of PI characters, missing data.

Alignment	No. of taxa	No. sites	Missing data (%)	No. of variable/Parsimony informative sites
Nuclear	47	392,600	13.2	43,250/18,057
Plastid	47	159,365	1.8	8,243/4,693

Table 2. Model selection of the different species networks and bifurcating trees.

					Information criteria		
Topology	lnL	Parameters	Loci	Number of hybridizations	AIC	AICc	BIC
15 taxa							
Nuclear ASTRAL	-6134.788576	27	241	N/A	12323.577153	12330.675744	12417.666670
Nuclear RAxML	-6137.811629	27	241	N/A	12329.623259	12336.721850	12423.712776
Plastid	-6427.555081	27	241	N/A	12909.110161	12916.208753	13003.199679
Network 1	-6079.839883	29	241	1	12217.679766	12225.926212	12318.738877
Network 2	**-6006.511111**	**31**	**241**	**2**	**12075.022221**	**12084.515044**	**12183.050926**
Network 3	-6079.836581	33	241	1	12225.673162	12236.513742	12340.671461
Network 4	-6038.368637	35	241	4	12146.737274	12159.029957	12268.705166
Network 5	-6088.526401	37	241	5	12251.052802	12264.905019	12379.990288

890

设置格式[HXW]: 缩进: 左侧: 0 毫米, 首行缩进: 0 字符

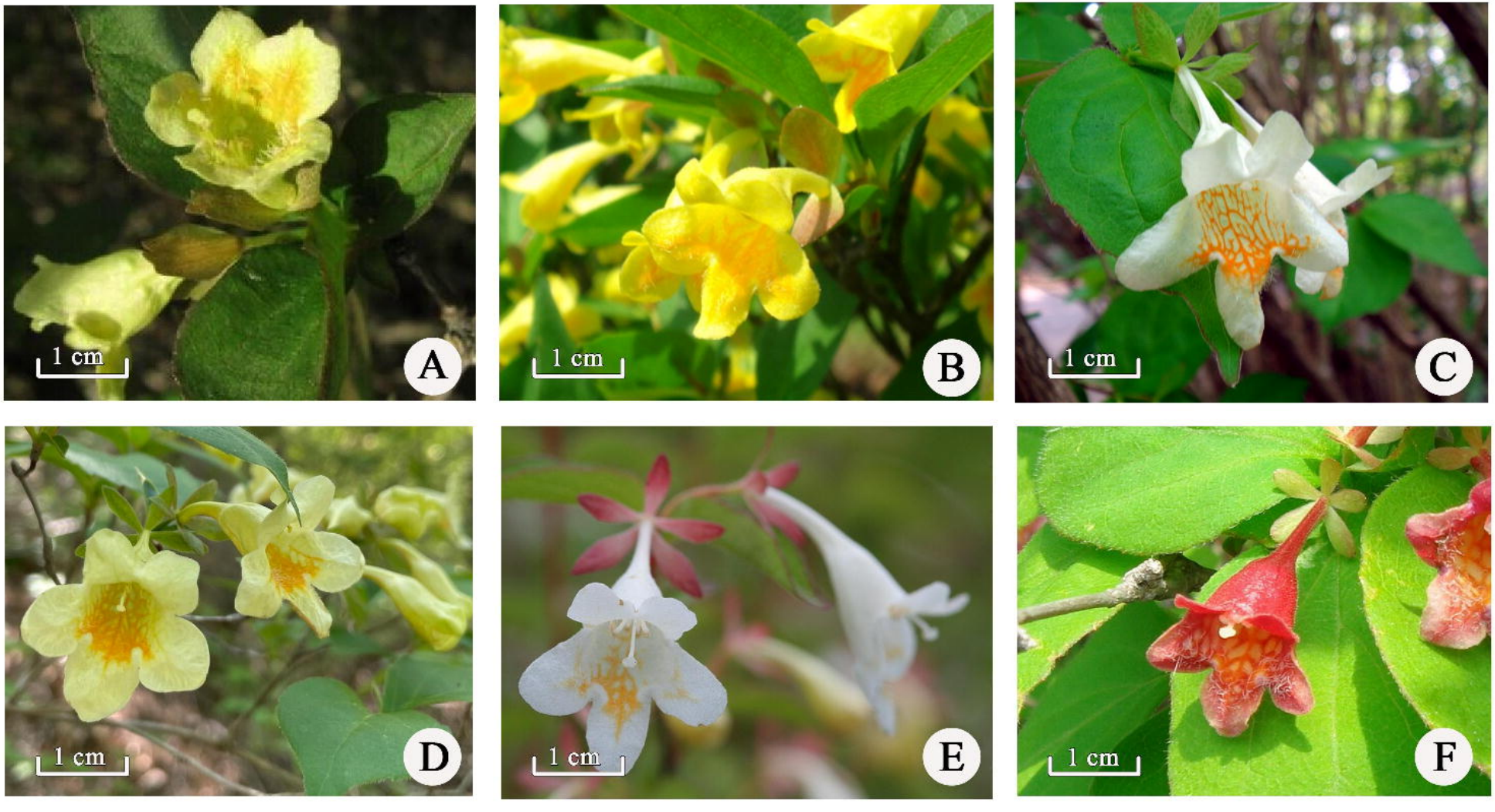
1 cm
A
1 cm
B
1 cm
C
1 cm
D
1 cm
E
1 cm
F

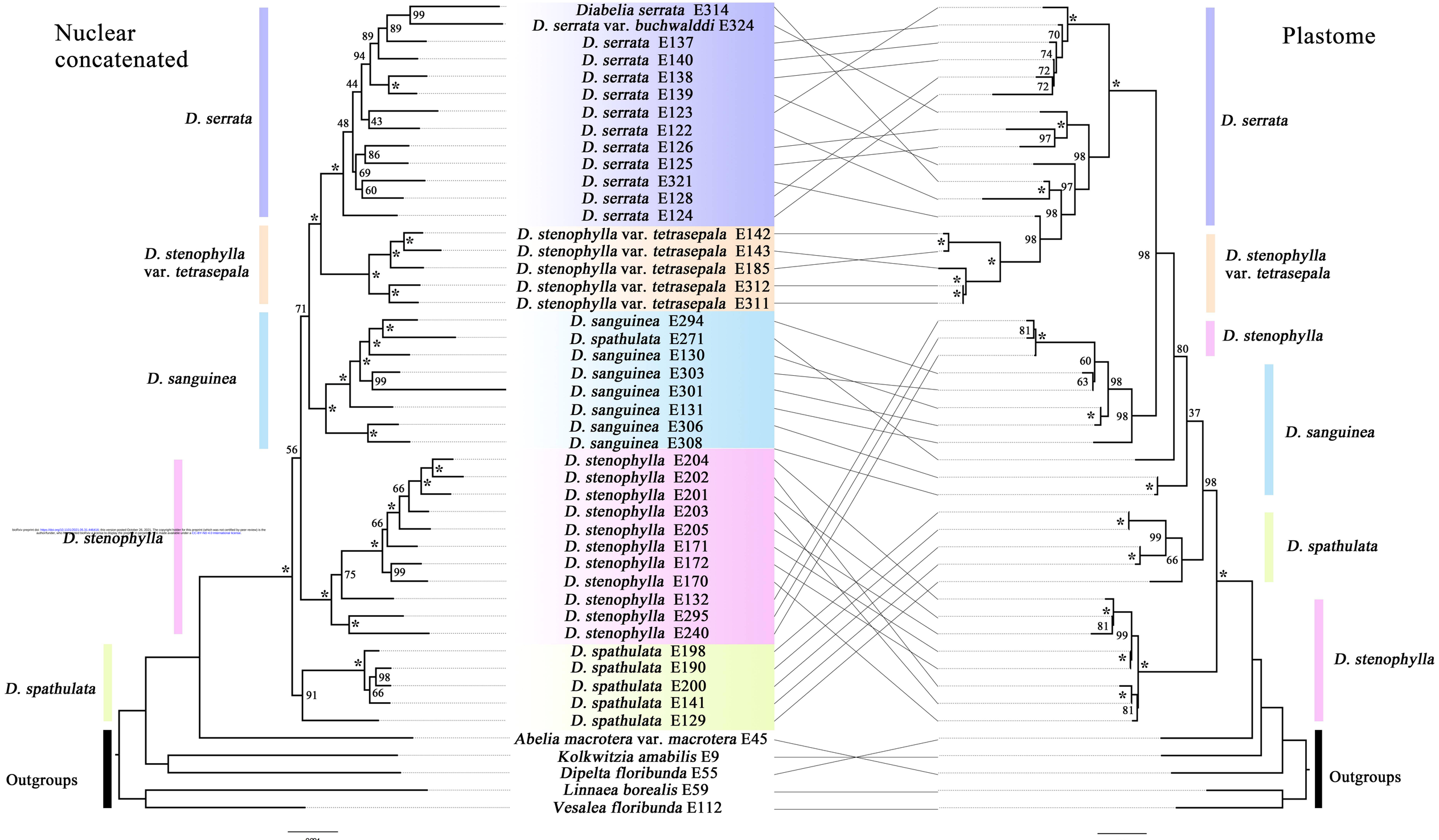

bioRxiv preprint doi: https://doi.org/10.1101/2021.05.31.446416; this version posted October 26, 2021. The copyright holder for this preprint (which was not certified by peer review) is the author/funder, who has granted bioRxiv a license to display the preprint in perpetuity. It is made available under a CC-BY-ND 4.0 International license.

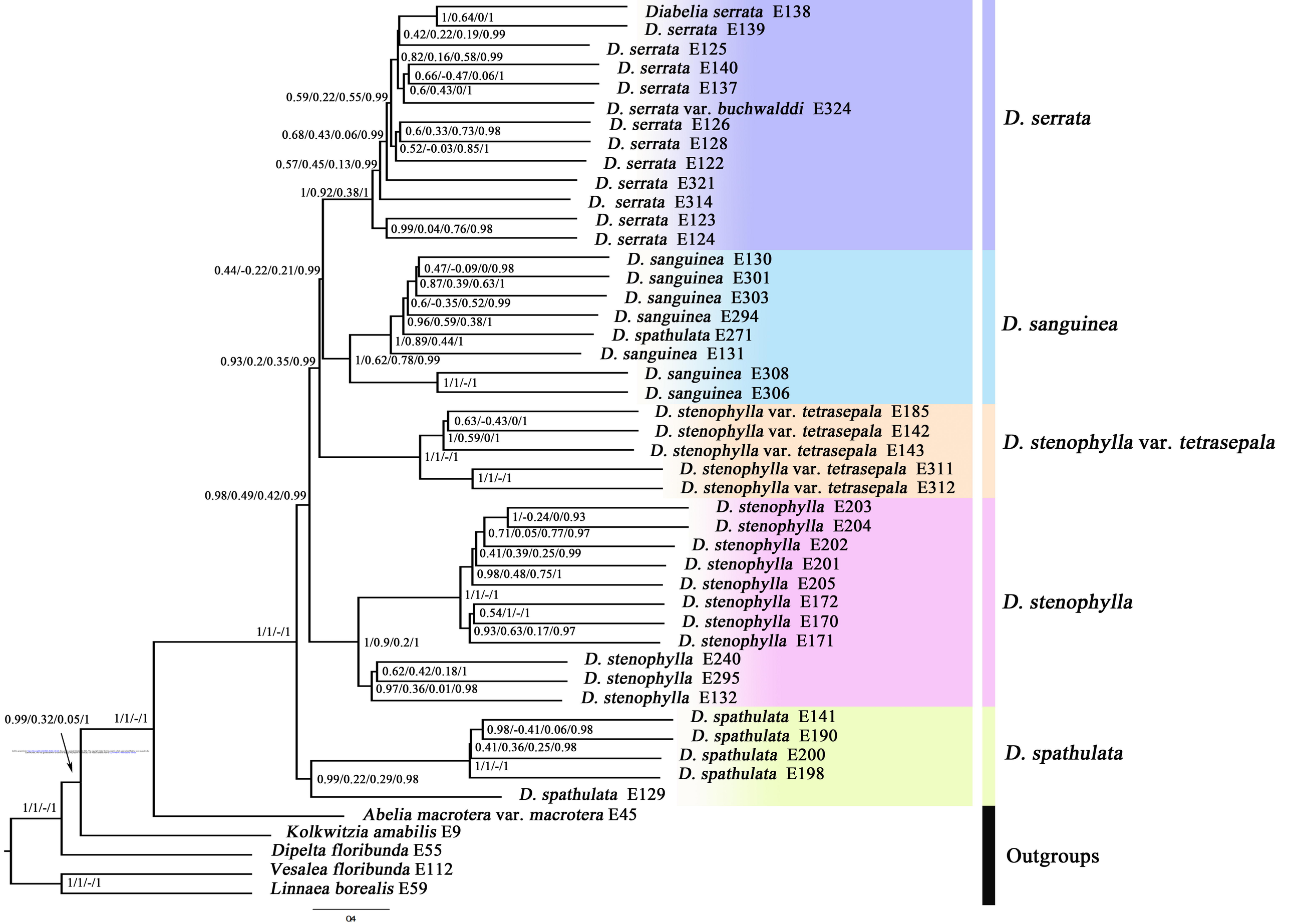
Diabelia serrata E138
D. serrata E139
D. serrata E125
D. serrata E140
D. serrata E137
D. serrata var. buchwalddi E324
D. serrata E126
D. serrata E128
D. serrata E122
D. serrata E321
D. serrata E314
D. serrata E123
D. serrata E124
D. sanguinea E130
D. sanguinea E301
D. sanguinea E303
D. sanguinea E294
D. spathulata E271
D. sanguinea E131
D. sanguinea E308
D. sanguinea E306
D. stenophylla var. tetrasepala E185
D. stenophylla var. tetrasepala E142
D. stenophylla var. tetrasepala E143
D. stenophylla var. tetrasepala E311
D. stenophylla var. tetrasepala E312
D. stenophylla E203
D. stenophylla E204
D. stenophylla E202
D. stenophylla E201
D. stenophylla E205
D. stenophylla E172
D. stenophylla E170
D. stenophylla E171
D. stenophylla E240
D. stenophylla E295
D. stenophylla E132
D. spathulata E141
D. spathulata E190
D. spathulata E200
D. spathulata E198
D. spathulata E129
Abelia macrotera var. macrotera E45
Kolkwitzia amabilis E9
Dipelta floribunda E55
Vesalea floribunda E112
Linnaea borealis E59
1/0.64/0/1
0.42/0.22/0.19/0.99
0.82/0.16/0.58/0.99
0.66/-0.47/0.06/1
0.6/0.43/0/1
0.59/0.22/0.55/0.99
0.6/0.33/0.73/0.98
0.52/-0.03/0.85/1
0.68/0.43/0.06/0.99
0.57/0.45/0.13/0.99
1/0.92/0.38/1
0.99/0.04/0.76/0.98
0.47/-0.09/0/0.98
0.87/0.39/0.63/1
0.6/-0.35/0.52/0.99
0.96/0.59/0.38/1
1/0.89/0.44/1
0.44/-0.22/0.21/0.99
1/0.62/0.78/0.99
0.93/0.2/0.35/0.99
1/1/-/1
0.63/-0.43/0/1
1/0.59/0/1
1/1/-/1
1/1/-/1
0.98/0.49/0.42/0.99
1/-0.24/0/0.93
0.71/0.05/0.77/0.97
0.41/0.39/0.25/0.99
0.98/0.48/0.75/1
1/1/-/1
0.54/1/-/1
0.93/0.63/0.17/0.97
1/0.9/0.2/1
1/1/-/1
0.62/0.42/0.18/1
0.97/0.36/0.01/0.98
0.99/0.32/0.05/1
1/1/-/1
0.98/-0.41/0.06/0.98
0.41/0.36/0.25/0.98
1/1/-/1
0.99/0.22/0.29/0.98
1/1/-/1
1/1/-/1
D. serrata
D. sanguinea
D. stenophylla var. tetrasepala
D. stenophylla
D. spathulata
Outgroups
04

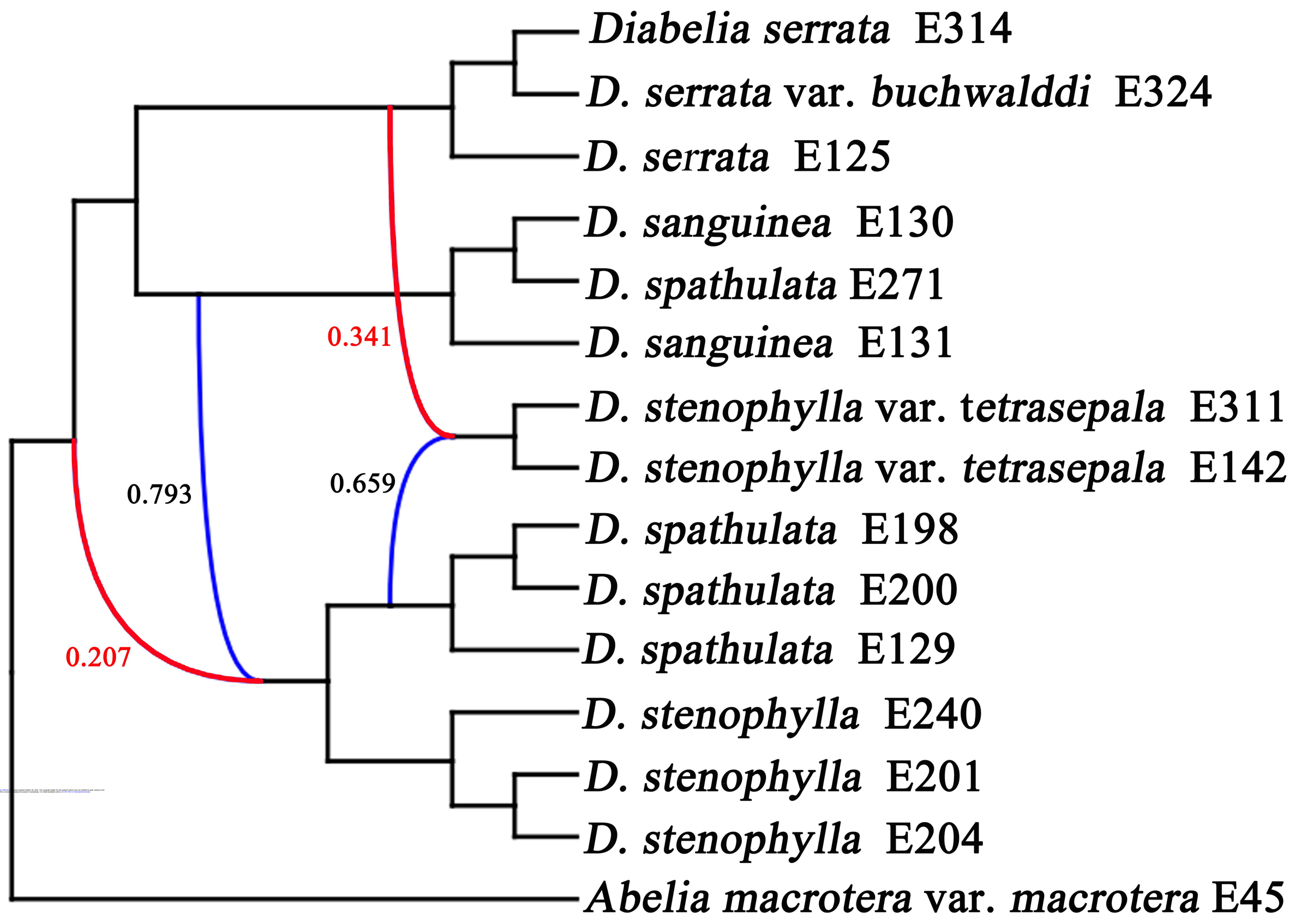

Diabelia serrata E314
D. serrata var. buchwalddi E324
D. serrata E125
D. sanguinea E130
D. spathulata E271
D. sanguinea E131
D. stenophylla var. tetrasepala E311
D. stenophylla var. tetrasepala E142
D. spathulata E198
D. spathulata E200
D. spathulata E129
D. stenophylla E240
D. stenophylla E201
D. stenophylla E204
Abelia macrotera var. macrotera E45
0.341
0.793
0.659
0.207

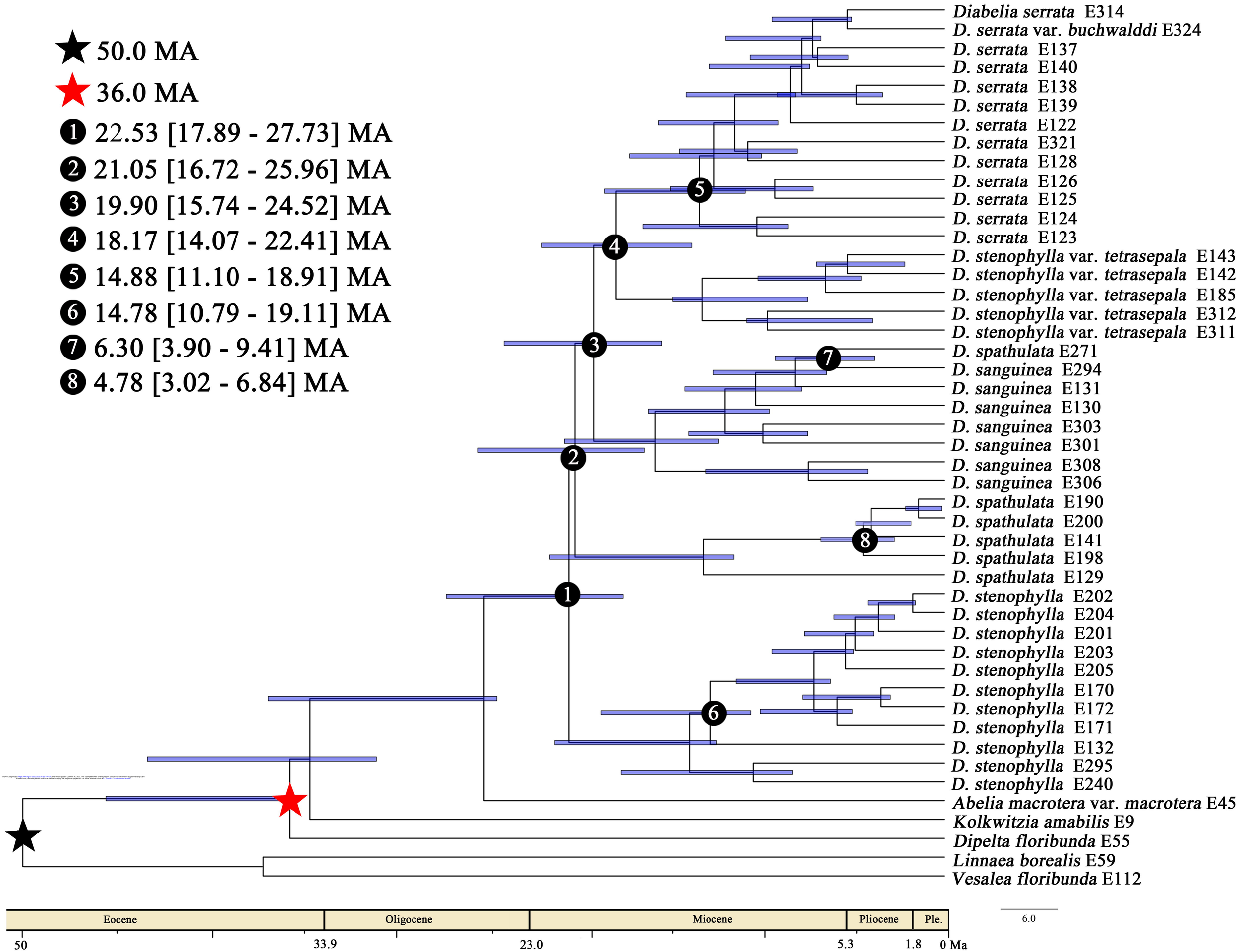
50.0 MA
36.0 MA
1 22.53 [17.89 - 27.73] MA
2 21.05 [16.72 - 25.96] MA
3 19.90 [15.74 - 24.52] MA
4 18.17 [14.07 - 22.41] MA
5 14.88 [11.10 - 18.91] MA
6 14.78 [10.79 - 19.11] MA
7 6.30 [3.90 - 9.41] MA
8 4.78 [3.02 - 6.84] MA
Diabelia serrata E314
D. serrata var. buchwalddi E324
D. serrata E137
D. serrata E140
D. serrata E138
D. serrata E139
D. serrata E122
D. serrata E321
D. serrata E128
D. serrata E126
D. serrata E125
D. serrata E124
D. serrata E123
D. stenophylla var. tetrasepala E143
D. stenophylla var. tetrasepala E142
D. stenophylla var. tetrasepala E185
D. stenophylla var. tetrasepala E312
D. stenophylla var. tetrasepala E311
D. spathulata E271
D. sanguinea E294
D. sanguinea E131
D. sanguinea E130
D. sanguinea E303
D. sanguinea E301
D. sanguinea E308
D. sanguinea E306
D. spathulata E190
D. spathulata E200
D. spathulata E141
D. spathulata E198
D. spathulata E129
D. stenophylla E202
D. stenophylla E204
D. stenophylla E201
D. stenophylla E203
D. stenophylla E205
D. stenophylla E170
D. stenophylla E172
D. stenophylla E171
D. stenophylla E132
D. stenophylla E295
D. stenophylla E240
Abelia macrotera var. macrotera E45
Kolkwitzia amabilis E9
Dipelta floribunda E55
Linnaea borealis E59
Vesalea floribunda E112
Eocene
Oligocene
Miocene
Pliocene
Ple.
50
33.9
23.0
5.3
1.8
0 Ma
6.0

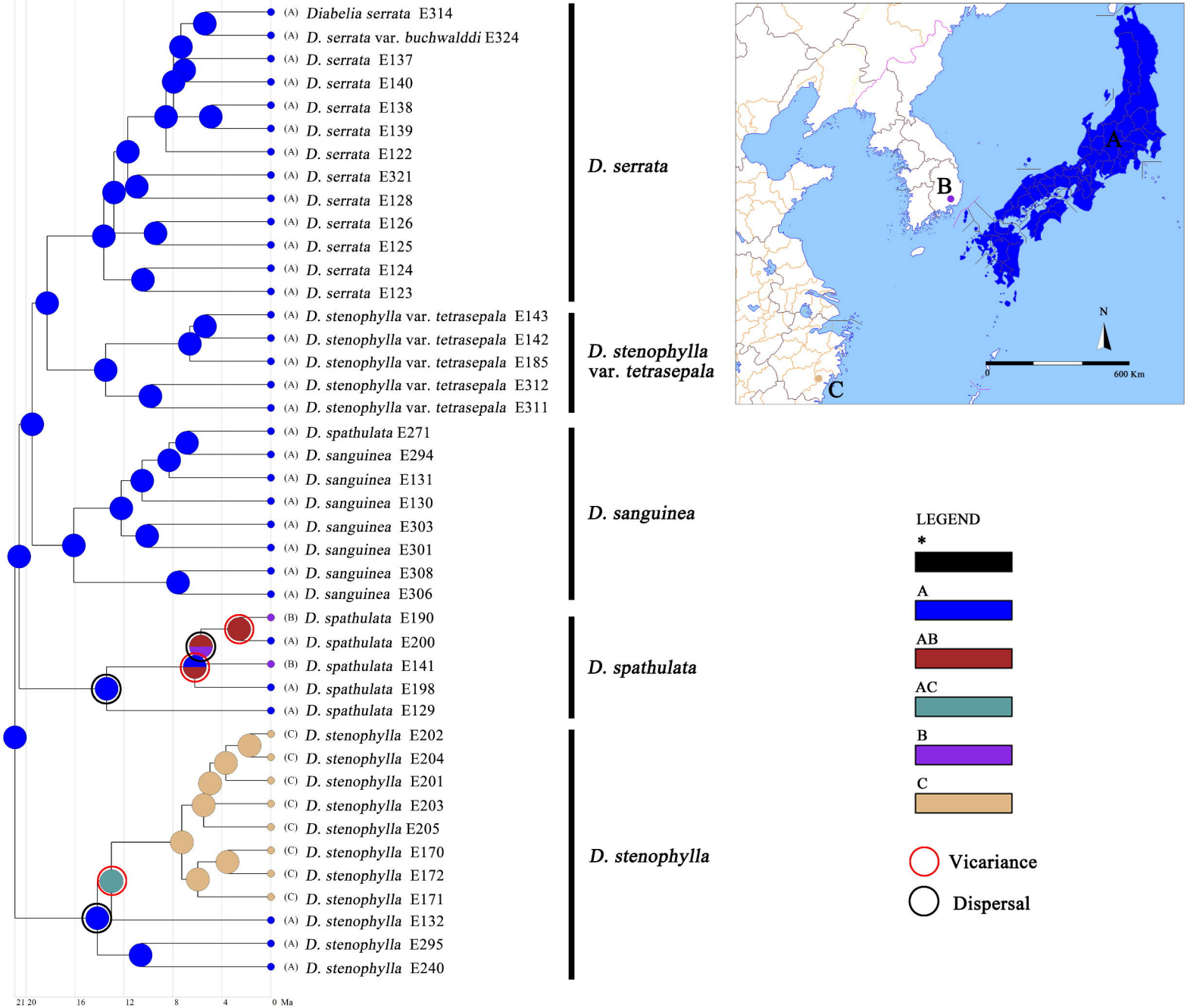
(A) Diabelia serrata E314
(A) D. serrata var. buchwalddi E324
(A) D. serrata E137
(A) D. serrata E140
(A) D. serrata E138
(A) D. serrata E139
(A) D. serrata E122
(A) D. serrata E321
(A) D. serrata E128
(A) D. serrata E126
(A) D. serrata E125
(A) D. serrata E124
(A) D. serrata E123
(A) D. stenophylla var. tetrasepala E143
(A) D. stenophylla var. tetrasepala E142
(A) D. stenophylla var. tetrasepala E185
(A) D. stenophylla var. tetrasepala E312
(A) D. stenophylla var. tetrasepala E311
(A) D. spathulata E271
(A) D. sanguinea E294
(A) D. sanguinea E131
(A) D. sanguinea E130
(A) D. sanguinea E303
(A) D. sanguinea E301
(A) D. sanguinea E308
(A) D. sanguinea E306
(B) D. spathulata E190
(A) D. spathulata E200
(B) D. spathulata E141
(A) D. spathulata E198
(A) D. spathulata E129
(C) D. stenophylla E202
(C) D. stenophylla E204
(C) D. stenophylla E201
(C) D. stenophylla E203
(C) D. stenophylla E205
(C) D. stenophylla E170
(C) D. stenophylla E172
(C) D. stenophylla E171
(A) D. stenophylla E132
(A) D. stenophylla E295
(A) D. stenophylla E240
D. serrata
D. stenophylla var. tetrasepala
D. sanguinea
D. spathulata
D. stenophylla
21 20 16 12 8 4 0 Ma
A
B
C
N
0
600 Km
LEGEND
*
A
AB
AC
B
C
Vicariance
Dispersal

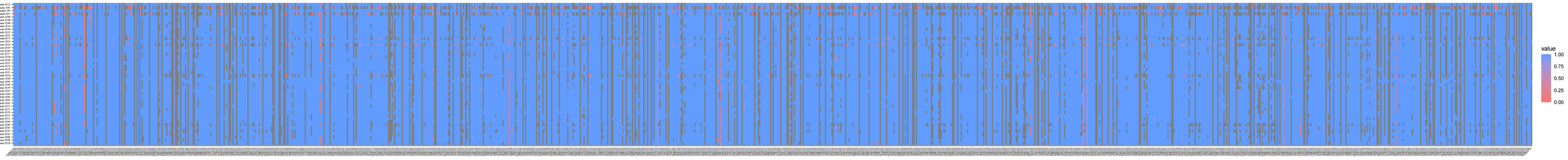
value
1.00
0.75
0.50
0.25
0.00

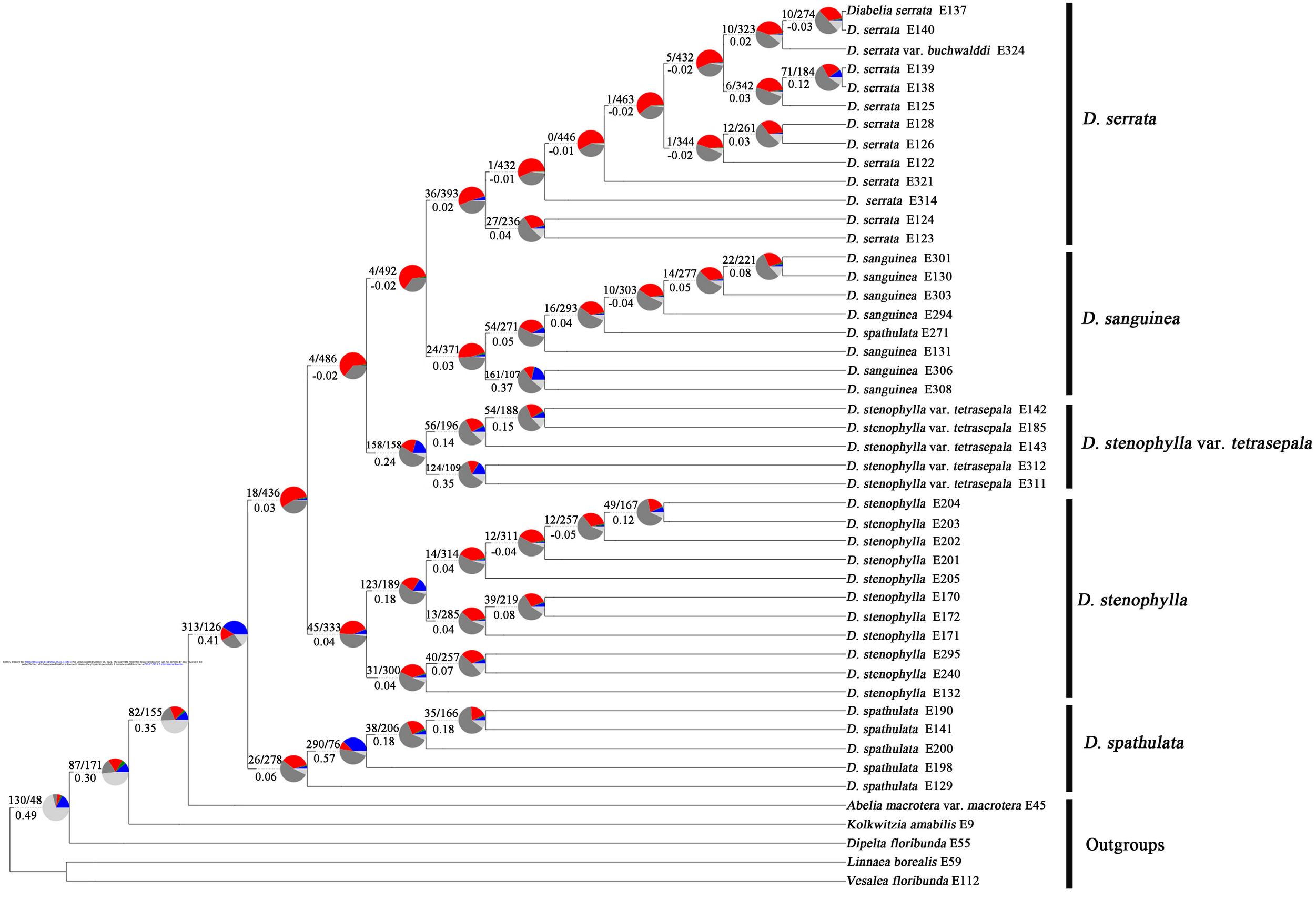

bioRxiv preprint doi: https://doi.org/10.1101/2021.05.31.446416; this version posted October 26, 2021. The copyright holder for this preprint (which was not certified by peer review) is the author/funder, who has granted bioRxiv a license to display the preprint in perpetuity. It is made available under a CC-BY-ND 4.0 International license.

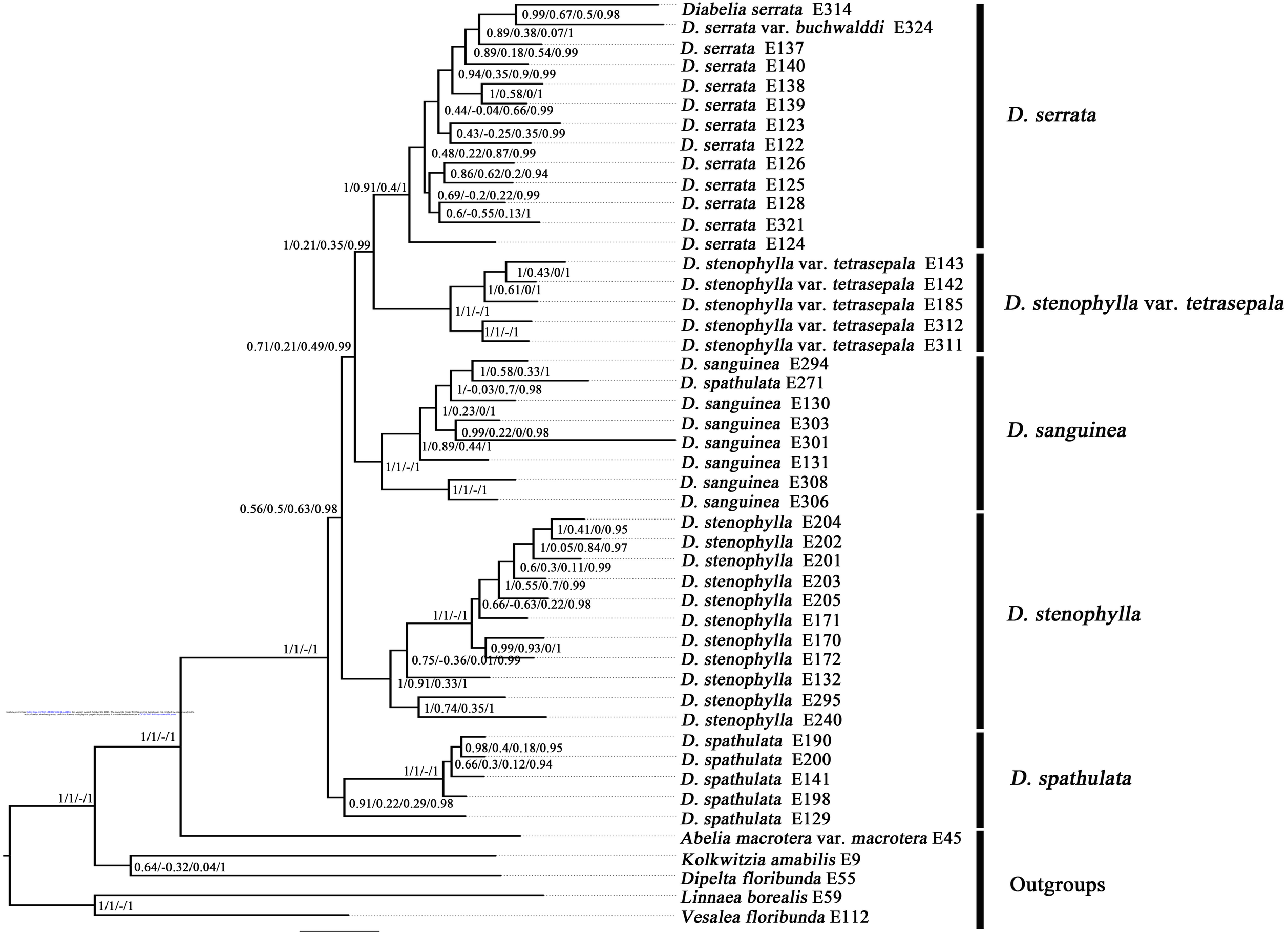

bioRxiv preprint doi: https://doi.org/10.1101/2021.05.31.446416; this version posted October 26, 2021. The copyright holder for this preprint (which was not certified by peer review) is the author/funder, who has granted bioRxiv a license to display the preprint in perpetuity. It is made available under a CC-BY-ND 4.0 International license.

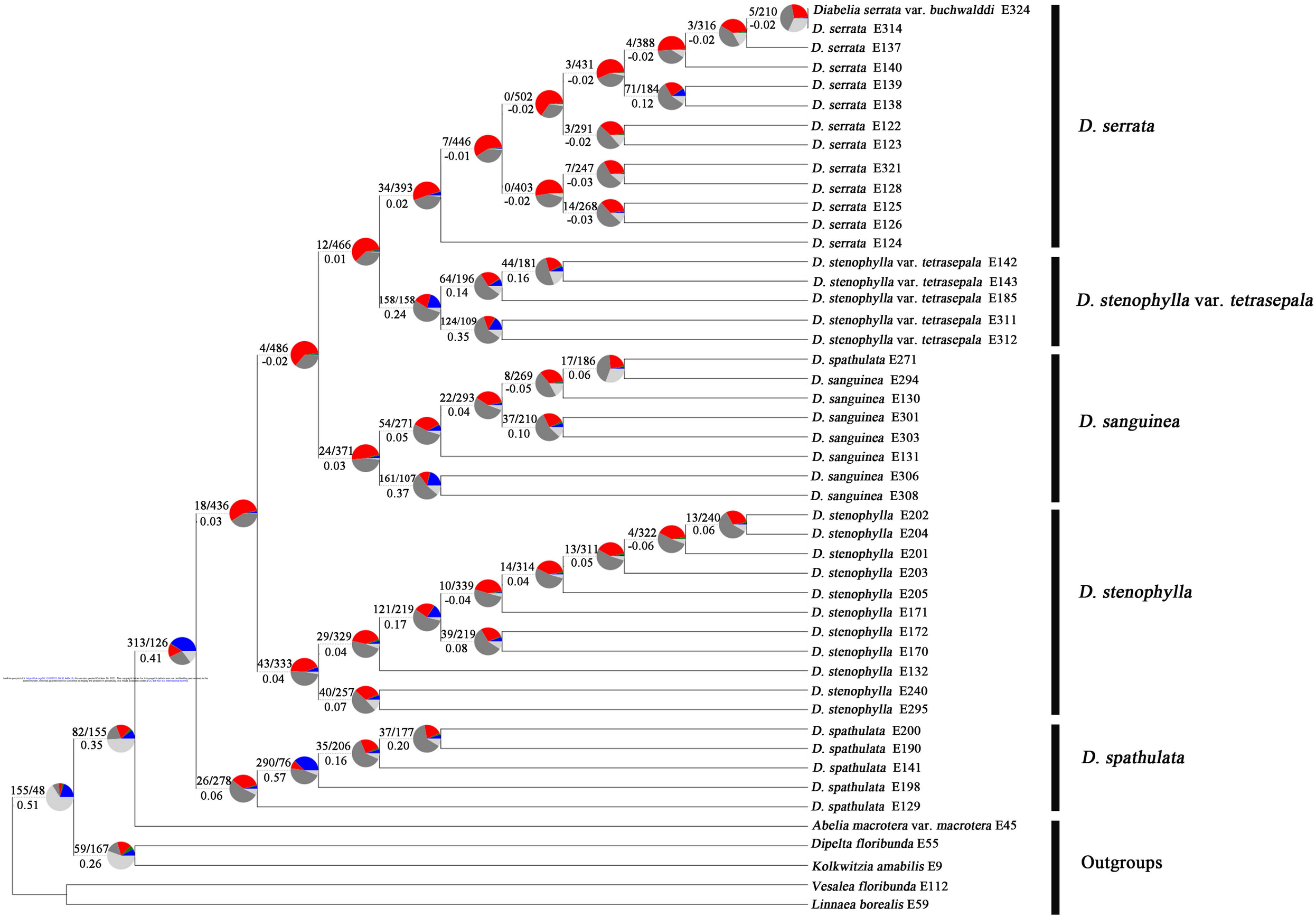

bioRxiv preprint doi: https://doi.org/10.1101/2021.05.31.446416; this version posted October 26, 2021. The copyright holder for this preprint (which was not certified by peer review) is the author/funder, who has granted bioRxiv a license to display the preprint in perpetuity. It is made available under a CC-BY-ND 4.0 International license.

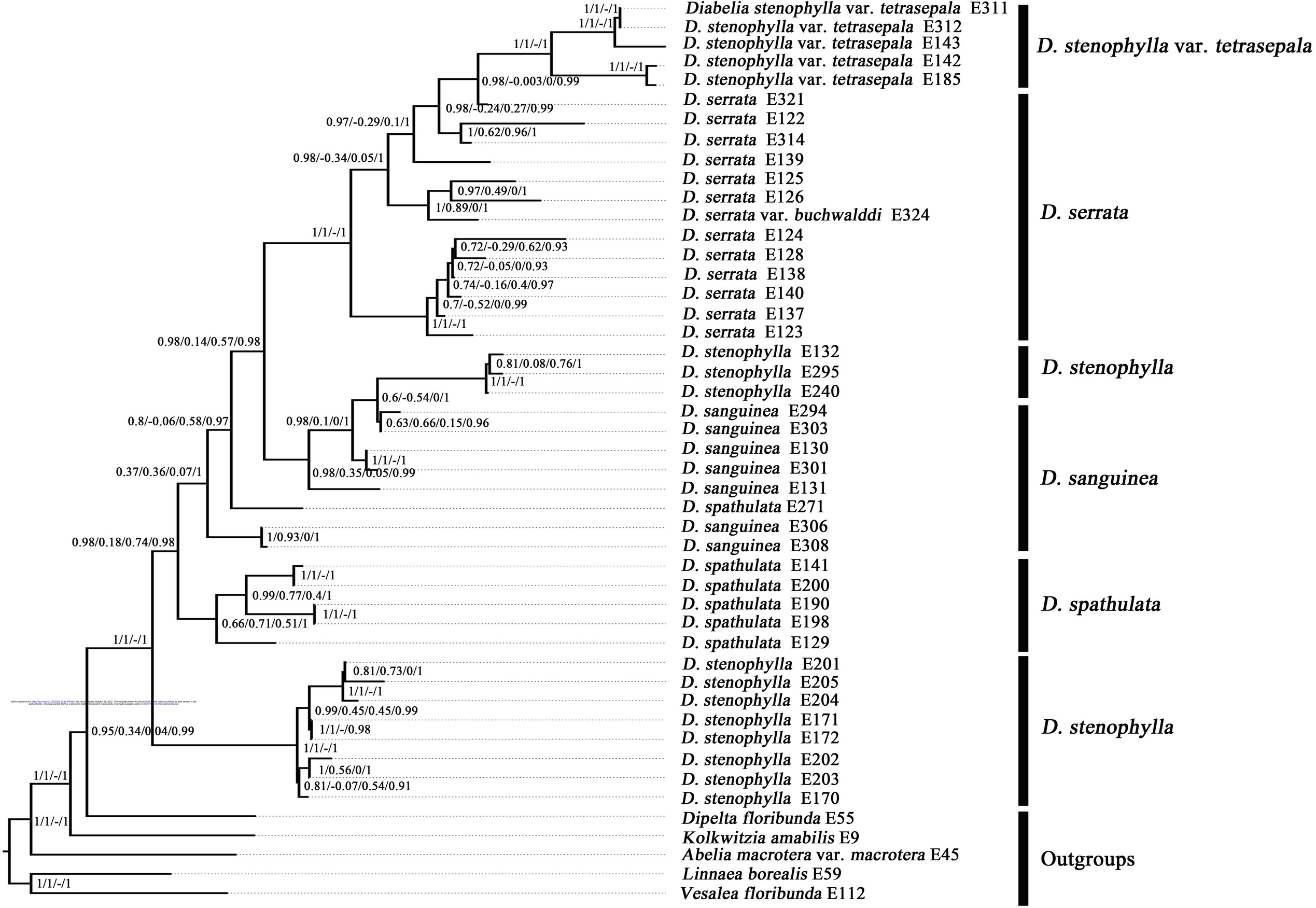

bioRxiv preprint doi: https://doi.org/10.1101/2021.05.31.446416; this version posted October 26, 2021. The copyright holder for this preprint (which was not certified by peer review) is the author/funder, who has granted bioRxiv a license to display the preprint in perpetuity. It is made available under a CC-BY-NC-ND 4.0 International license.

bioRxiv preprint doi: https://doi.org/10.1101/2021.05.31.446416; this version posted October 26, 2021. The copyright holder for this preprint (which was not certified by peer review) is the author/funder, who has granted bioRxiv a license to display the preprint in perpetuity. It is made available under a CC-BY-ND 4.0 International license.

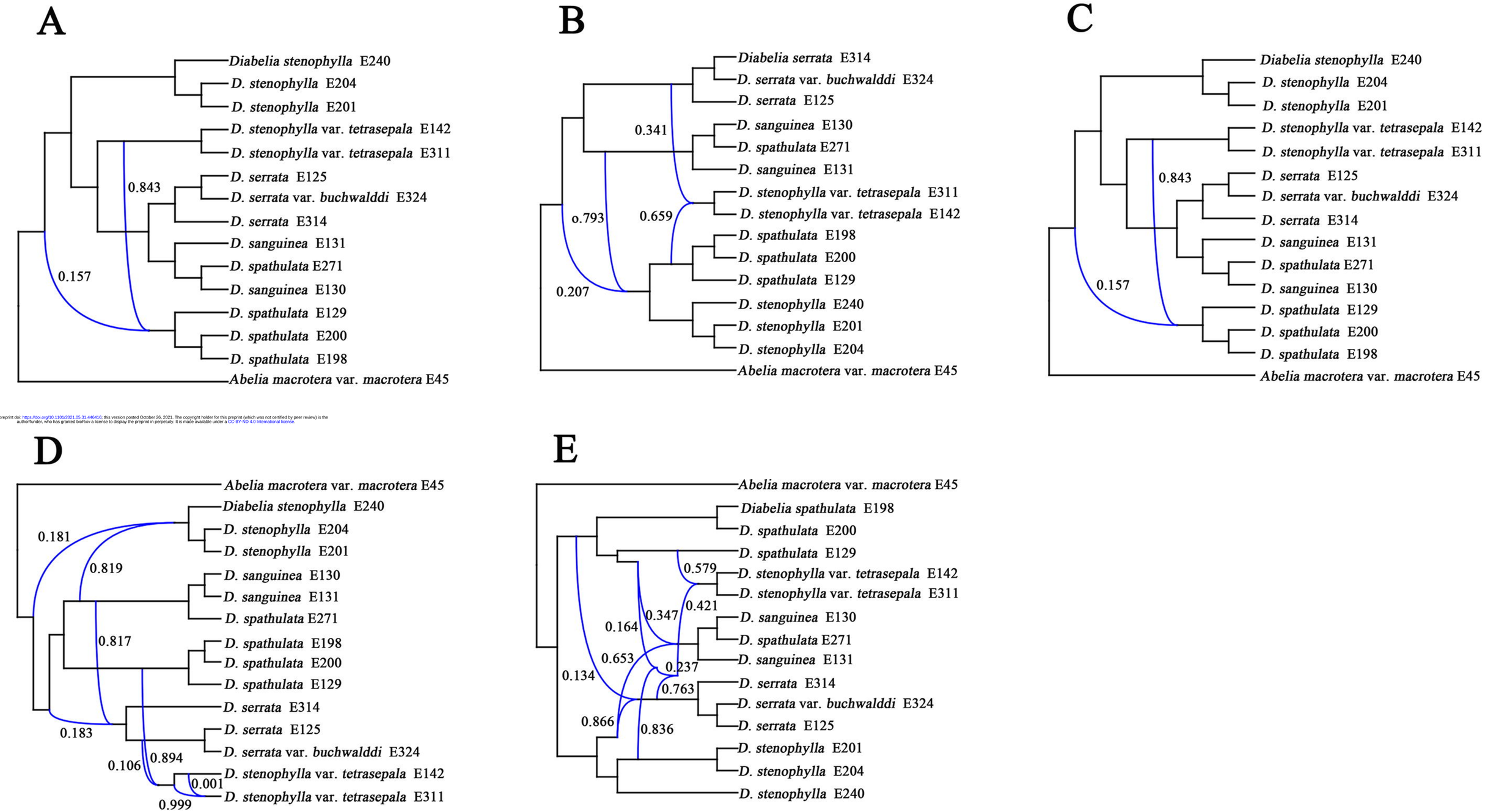

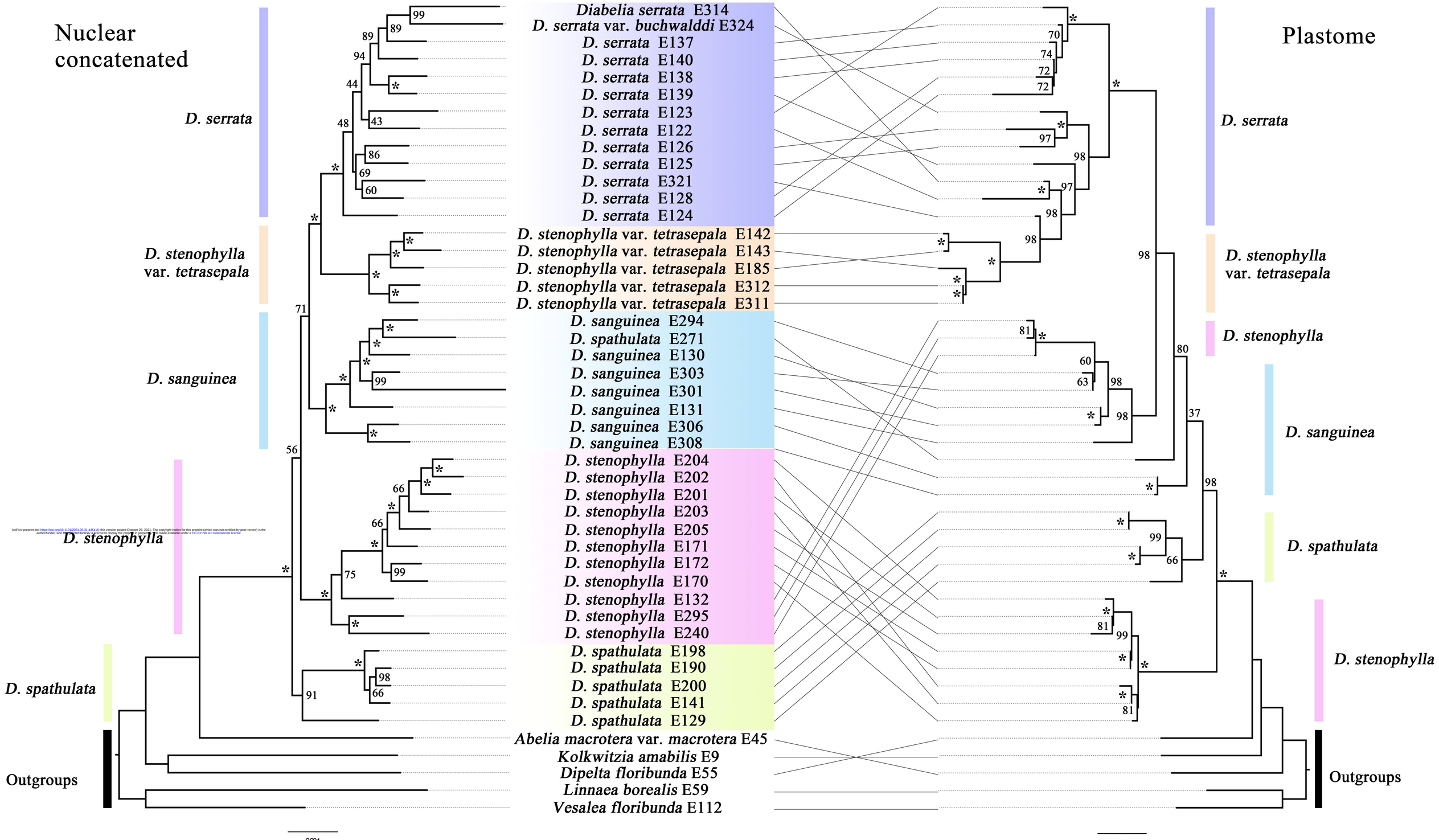

bioRxiv preprint doi: https://doi.org/10.1101/2021.05.31.446416; this version posted October 26, 2021. The copyright holder for this preprint (which was not certified by peer review) is the author/funder, who has granted bioRxiv a license to display the preprint in perpetuity. It is made available under a CC-BY-ND 4.0 International license.

Table. S1 **List of species and vouchers used in this study.**

Order	Ingroup/ Outgroup	Taxon	Coding	Locality	Voucher specimen number	SRA accession
1	Ingroup	*Diabelia serrata*	A	Ogawara plateau,Tokushima , Japan	HUTB, E314	SRR15731354
2	Ingroup	*Diabelia serrata* var. *buchwaddi*	A	Takanose-kyo gorge, Kito, Naka-cho, Kochi, Japan	HUTB, E324	SRR15731353
3	Ingroup	*Diabelia serrata*	A	Mt. Shiraga, Motoyama-cho, Kochi, Japan	HUTB, E137	SRR15731342
4	Ingroup	*Diabelia serrata*	A	Kochi, Japan	HUTB, E140	SRR15731331
5	Ingroup	*Diabelia serrata*	A	Kakiki-mura, Kanoashi-gun, Shimane, Japan	HUTB, E122	SRR15731324
6	Ingroup	*Diabelia serrata*	A	Anan, Tokushima, Japan	HUTB, E123	SRR13705758
7	Ingroup	*Diabelia serrata*	A	Mt. Shiraga, Motoyama-cho, Kochi, Japan	HUTB, E138	SRR15731323
8	Ingroup	*Diabelia serrata*	A	Mt. Shiraga, Motoyama-cho, Kochi, Japan	HUTB, E139	SRR15731322
9	Ingroup	*Diabelia serrata*	A	Takanose-kyo gorge, Kito, Naka-cho, Kochi, Japan	HUTB, E128	SRR15731321
10	Ingroup	*Diabelia serrata*	A	Takakuma, Kagoshima, Japan	HUTB, E321	SRR13890747
11	Ingroup	*Diabelia serrata*	A	Mt. Shozanji, Kamiyama, Tokushima, Japan	HUTB, E125	SRR15731320
12	Ingroup	*Diabelia serrata*	A	Ogawara plateau,Tokushima , Japan	HUTB, E126	SRR15731319
13	Ingroup	*Diabelia serrata*	A	Takaga, Seki city, Gifu, Japan	HUTB, E124	SRR15731352
14	Ingroup	*Diabelia stenophylla var. tetrasepala*	A	Mt. Takamaru, Kamikatsu, Tokushima, Japan	HUTB, E142	SRR15731351
15	Ingroup	*Diabelia stenophylla var. tetrasepala*	A	Mt. Takamaru, Kamikatsu, Tokushima, Japan	HUTB, E143	SRR15731350
16	Ingroup	*Diabelia stenophylla var. tetrasepala*	A	Mt. Takamaru, Kamikatsu, Tokushima, Japan	HUTB, E185	SRR15731349
17	Ingroup	*Diabelia stenophylla var. tetrasepala*	A	Mt. Takamaru, Kamikatsu, Tokushima, Japan	HUTB, E312	SRR15731348
18	Ingroup	*Diabelia stenophylla var. tetrasepala*	A	Mt. Takamaru, Kamikatsu, Tokushima, Japan	HUTB, E311	SRR15731347
19	Ingroup	*Diabelia spathulata*	A	Tochigi, Japan	HUTB, E271	SRR15731346
20	Ingroup	*Diabelia sanguinea*	A	Yumoto, Nasu-cho, Nasu-gun, Tochigi, Japan	HUTB, E130	SRR15731345

21	Ingroup	*Diabelia sanguinea*	A	Mt. Takamaru, Kamikatsu, Tokushima, Japan	HUTB, E294	SRR15731344
22	Ingroup	*Diabelia sanguinea*	A	Zike, Toyama city, Toyama, Japan	HUTB, E131	SRR15731343
23	Ingroup	*Diabelia sanguinea*	A	Sendai, Miyagi, Japan	HUTB, E301	SRR13705755
24	Ingroup	*Diabelia sanguinea*	A	Mt. Kinkan, Numadzu city, Shizuoka, Japan	HUTB, E303	SRR13890746
25	Ingroup	*Diabelia sanguinea*	A	Tanyama, Nagano, Japan	HUTB, E308	SRR15731341
26	Ingroup	*Diabelia sanguinea*	A	Tanyama, Nagano, Japan	HUTB, E306	SRR13705756
27	Ingroup	*Diabelia spathulata*	B	Naewon temple forests,Yangsan-si, Gyeongsangnam-do, Korea	HUTB, E190	SRR15731340
28	Ingroup	*Diabelia spathulata*	A	Kowaki-cho, Higashiomi city, Shiga, Japan	HUTB, E200	SRR15731339
29	Ingroup	*Diabelia spathulata*	B	Naewon temple forests,Yangsan-si, Gyeongsangnam-do, Korea	HUTB, E141	SRR15731338
30	Ingroup	*Diabelia spathulata*	A	Kowaki-cho, Higashiomi city, Shiga, Japan	HUTB, E198	SRR13705757
31	Ingroup	*Diabelia spathulata*	A	Hatasawa, Obanasawa city, Yamagata, Japan	HUTB, E129	SRR15731337
32	Ingroup	*Diabelia stenophylla*	C	Wenzhou, Zhejiang, China	HUTB, E204	SRR13705754
33	Ingroup	*Diabelia stenophylla*	C	Wenzhou, Zhejiang, China	HUTB, E203	SRR15731336
34	Ingroup	*Diabelia stenophylla*	C	Wenzhou, Zhejiang, China	HUTB, E201	SRR15731335
35	Ingroup	*Diabelia stenophylla*	C	Wenzhou, Zhejiang, China	HUTB, E202	SRR15731334
36	Ingroup	*Diabelia stenophylla*	C	Wenzhou, Zhejiang, China	HUTB, E205	SRR15731333
37	Ingroup	*Diabelia stenophylla*	C	Wenzhou, Zhejiang, China	HUTB, E170	SRR15731332
38	Ingroup	*Diabelia stenophylla*	C	Wenzhou, Zhejiang, China	HUTB, E172	SRR15731330
39	Ingroup	*Diabelia stenophylla*	C	Wenzhou, Zhejiang, China	HUTB, E171	SRR15731329
40	Ingroup	*Diabelia stenophylla*	A	Saitama, Japan	HUTB, E240	SRR15731328
41	Ingroup	*Diabelia stenophylla*	A	Tabitomachi, Iwaki-shi, Fukushima Pref, Japan	HUTB, E295	SRR15731327
42	Ingroup	*Diabelia stenophylla*	A	Kami-sanbonmatsu, Honzyuku-cho, Okazaki city, Aichi, Japan	HUTB, E132	SRR15731326
43	Outgroup	*Abelia macrotera* var. *macrotera*		Yichang, Hubei, China	HUTB, E45	SRR13890750

44	Outgroup	*Dipelta floribunda*	Cambridge, UK.	HUTB, E55	SRR13705794
45	Outgroup	*Kolkwitzia amabilis*	Weinan, Shanxi, China	HUTB, E9	SRR13705797
46	Outgroup	*Vesalea floribunda*	Oaxaca, Mexico	HUTB, E112	SRR15731325
47	Outgroup	*Linnaea borealis*	Yili, Xinjiang, China	HUTB, E59	SRR13705788

Table S2. HybPiper assembly statistics

Species	Number of reads	Number of reads on target	Percent reads on target	Number of exons with reads	Number of exons with contigs	Number of exons with sequences	Number of exons with sequences > 25% of the target length	Number of exons with sequences > 50% of the target length	Number of exons with sequences > 75% of the target length	Number of exons with sequences > 150% of the target length	Number of exons with paralog warnings
D. spathulata E129	16390784	4958995	0.303	1114	1025	994	992	982	934	1	101
D. sanguinea E306	9313351	1888267	0.203	1119	1007	977	974	960	889	0	79
D. sanguinea E308	5571741	780542	0.14	1097	981	960	956	936	875	0	69
D. stenophylla var. tetrasepala E142	14145605	1023090	0.072	1089	987	963	962	952	899	1	79
D. stenophylla var. tetrasepala E143	4395804	228392	0.052	1050	900	878	878	851	783	0	54
D. stenophylla var. tetrasepala E185	5533465	1430420	0.259	1114	1008	978	977	959	898	0	90
D. sanguinea E294	1071353	238126	0.222	1021	876	862	861	841	779	0	56
D. stenophylla E295	9507905	2627497	0.276	1138	1024	992	992	971	904	0	92
D. tetrasepala E311	12638082	3514670	0.278	1144	1030	995	994	982	937	2	98
D. tetrasepala E312	26768128	7923496	0.296	1130	1022	995	994	984	940	2	102
D. stenophylla E170	8333538	2519416	0.302	1127	1017	995	994	979	922	1	90
D. stenophylla E171	8838954	2672116	0.302	1108	1017	987	985	972	923	1	96
D. stenophylla E172	6849894	2064638	0.301	1103	1008	983	981	962	908	1	92
D. stenophylla E201	10281957	3225974	0.314	1112	1015	988	987	973	922	1	86
D. stenophylla E202	7944302	2326039	0.293	1109	1012	986	985	968	915	1	86
D. stenophylla E203	8895646	3097609	0.348	1122	1022	996	995	980	924	1	85
D. stenophylla E204	6642696	2077347	0.313	1103	1006	983	982	962	908	1	76
D. stenophylla E205	9630997	2810192	0.292	1128	1020	995	993	972	920	1	80

D. sanguinea E130	4766791	879875	0.185	1065	981	958	956	942	887	0	79
D. stenophylla E240	8121657	922592	0.114	1098	988	963	961	933	838	0	66
D. sanguinea E301	12028399	2724711	0.227	1151	1062	1032	1032	1021	989	3	619
D. sanguinea E303	10970170	3075238	0.28	1134	1025	991	988	973	914	0	91
D. serrata var. *buchwaddi* E324	6665872	419228	0.063	1093	872	852	849	803	683	0	39
D. serrata E122	5880405	1892938	0.322	1064	999	978	977	962	895	0	85
D. serrata E123	21639680	7331755	0.339	1120	1033	998	996	980	933	1	136
D. serrata E124	22914349	9714647	0.424	1116	1031	1000	999	984	940	2	97
D. serrata E125	15011394	6415541	0.427	1105	1034	1003	1002	986	938	0	88
D. serrata E126	30652021	9145847	0.298	1124	1028	1002	1000	984	937	0	112
D. serrata E128	13934333	2581418	0.185	1091	999	975	974	959	909	1	102
D. serrata E137	4273733	735627	0.172	1060	974	952	950	933	871	0	79
D. serrata E138	14148609	3912863	0.277	1100	1020	993	992	979	924	1	83
D. serrata E139	10112962	2465780	0.244	1102	1002	983	982	968	910	0	96
D. serrata E314	5056940	378381	0.075	1050	877	850	839	746	587	1	36
D. serrata E321	13220295	4190116	0.317	1138	1037	1002	1000	986	934	0	93
D. spathulata E271	3089596	212920	0.069	992	827	809	806	762	661	0	39
D. sanguinea E131	13699360	3897086	0.284	1107	1018	991	990	979	930	1	87
D. stenophylla E132	7051574	1749371	0.248	1081	1000	976	974	958	905	1	86
D. serrata E140	6481952	1399052	0.216	1081	992	967	966	949	888	0	88
D. spathulata E141	6471860	1497704	0.231	1075	992	966	965	952	900	0	87
D. spathulata E190	8953298	2806002	0.313	1124	1022	989	986	973	928	2	86
D. spathulata E198	9267804	3459777	0.373	1130	1022	993	992	981	928	1	92
D. spathulata E200	8307344	2742274	0.33	1118	1018	991	990	980	922	1	86
Abelia macrotera var. *macrotera* E45	1833543	32422	0.018	825	436	424	417	355	253	0	6

Dipelta floribunda E55	4636783	105360	0.023	924	660	642	639	601	507	0	27
Kolkwitzia amabilis E9	9779050	2641147	0.27	1097	1005	984	983	967	916	0	75
Linnaea borealis E59	3831881	51899	0.014	867	536	516	507	443	333	0	11
Vesalea floribunda E112	3834861	805440	0.21	1061	970	947	946	915	856	0	52